Chapter 5

Within the Water

Once photons from the sun and sky have passed through the air-water surface, they initiate a complex chain of scattering and absorption events within the water body. The primary goal of this chapter is to develop the basic equation, known as the *radiance transfer equation,* governing the behavior of radiance within natural water bodies. This equation, when combined with the boundary conditions developed in the previous chapter, gives us the ability to predict underwater radiance distributions given the water's inherent optical properties, the incident lighting, and the sea state. The radiance transfer equation also yields a set of equations governing the irradiances.

These equations are the theoretical framework for predicting and interpreting underwater light fields in terms of the physical, chemical and biological constituents of natural water bodies. In addition, the equations are the basis for various *inverse models*, which attempt to recover inherent optical properties from measured radiometric quantities.

Many approaches can be taken in deriving the radiance transfer equation, which we shall call the "RTE" for convenience. We stated at the beginning of Chapter 4 that all of radiative transfer theory can be based on the concept of linear interaction principles. Indeed, Preisendorfer (1965, Sections 125-126) outlines how to start with Maxwell's equations, which govern electromagnetic fields, and arrive at an appropriate interaction principle for radiance within a medium. He then shows how that interaction principle leads to the RTE. These matters are treated with mathematical rigor in *H.O. II.* This approach to the RTE is philosophically parallel to our use of interaction principles in discussing radiative transfer across the air-water surface. Unfortunately, though, this approach is more mathematical and less physically revealing than was the development in Chapter 4.

Measures (1992) derives the RTE beginning with quantum mechanical descriptions of absorption, scattering and emission. This approach is physically revealing because it connects the macroscopic, phenomenological viewpoint with the microscopic, physical properties of the atoms and molecules forming the natural water body. However, this derivation requires a fairly sophisticated understanding of quantum mechanics. Stamnes (1986) starts with the concept of a photon gas and

derives the RTE from a more general Boltzmann equation. Fante (1981) shows how to proceed rigorously from Maxwell's equations to the RTE. It is also possible to proceed directly from the laws of quantum electrodynamics and arrive at the RTE (Acquista and Anderson, 1977), but this approach is very abstract.

We shall pursue yet another approach to the RTE. Our development is intuitive, mathematically simple, physically revealing, and consistent with our phenomenological treatment of radiative transfer theory.

5.1 Radiative Processes

When a photon interacts with an atom or molecule, the photon may be absorbed, leaving the atom or molecule in a state with higher internal (electronic, vibrational, or rotational) energy. If the molecule (say) almost immediately returns to its original internal energy state by emitting a photon of the same energy as the absorbed photon, the process is called *elastic scattering*.

However, the excited molecule may emit a photon of less energy (longer wavelength) than the incident photon. The molecule thus remains in an intermediate excited state and may at a later time emit another photon and return to its original state, or the retained energy may be converted to thermal or chemical energy. Indeed, if the molecule is initially in an excited state, it may absorb the incident photon and then emit a photon of greater energy (shorter wavelength) than the absorbed photon, thereby returning to a lower energy state. In either case the scattered (emitted) photon has a different wavelength than the incident (absorbed) photon, and the processes is called *inelastic*, or *transpectral*, *scattering* [see Supplementary Note 7].

Finally, all or part of the absorbed photon's energy may be converted into thermal (kinetic) energy, or into chemical energy (manifested, for example, in the formation of new chemical compounds). The conversion of a photon's energy into a nonradiant form is called *true absorption*. The reverse process is also possible, as when chemical energy is converted into light; this process is called *true emission.*

In order to formulate the radiance transfer equation, it is convenient to imagine light in the form of many beams of photons coursing in all directions through each point of a water body, and to think of all the ways in which each beam's population of photons may be decreased or increased. Bearing in mind the preceding comments, the following six processes are both necessary and sufficient to write down an energy balance equation for a beam of photons on the phenomenological level:

(i)   loss of photons from the beam through scattering to other directions without change in wavelength (elastic scattering)

(ii)   loss of photons from the beam through scattering (perhaps to other directions) with change in wavelength (inelastic scattering)

(iii)   loss of photons from the beam through annihilation of photons by conversion of radiant energy to nonradiant energy (true absorption)

(iv)   gain of photons by the beam through scattering (from other directions) without change in wavelength (elastic scattering)

(v)   gain of photons by the beam through scattering (perhaps from other directions) with change in wavelength (inelastic scattering)

(vi)   gain of photons by the beam through creation of photons by conversion of nonradiant energy into radiant energy (true emission)

These processes in turn will now be given quantitative forms as needed for the equation of transfer.

5.2 Elastic Scattering

We already have defined the spectral volume scattering function (VSF) for elastic scattering, $\beta(\psi,\lambda)$ [recall Fig. 3.1 and Eq. (3.4)]. We assumed in that discussion that there was no change in wavelength induced by the scattering process and that the scattering depended only on the angle ψ between the incident photon direction $\hat{\xi}'$ and the final photon direction $\hat{\xi}$. We now re-examine the scattering process with the goal of obtaining a mathematical description of radiative process (iv), the increase of radiance in a collimated beam owing to elastic scattering.

The path function for elastic scattering

Figure 5.1 shows an experimental setup for *in situ* measurement of scattering. A monochromator-collimator device shoots a narrow beam of unpolarized radiant power of wavelength $\lambda \equiv \lambda'$ from source point S to point $\vec{x}$ and beyond in the scattering-absorbing medium. Here "$\vec{x}$" simply denotes a location in the water, somewhere along the beam. Photons are being absorbed and scattered by the medium all along the extent of the beam. The scattering activity at point $\vec{x}$ of the beam is examined in detail by a radiance meter located at the detector point D. The narrow beam from S to $\vec{x}$ and
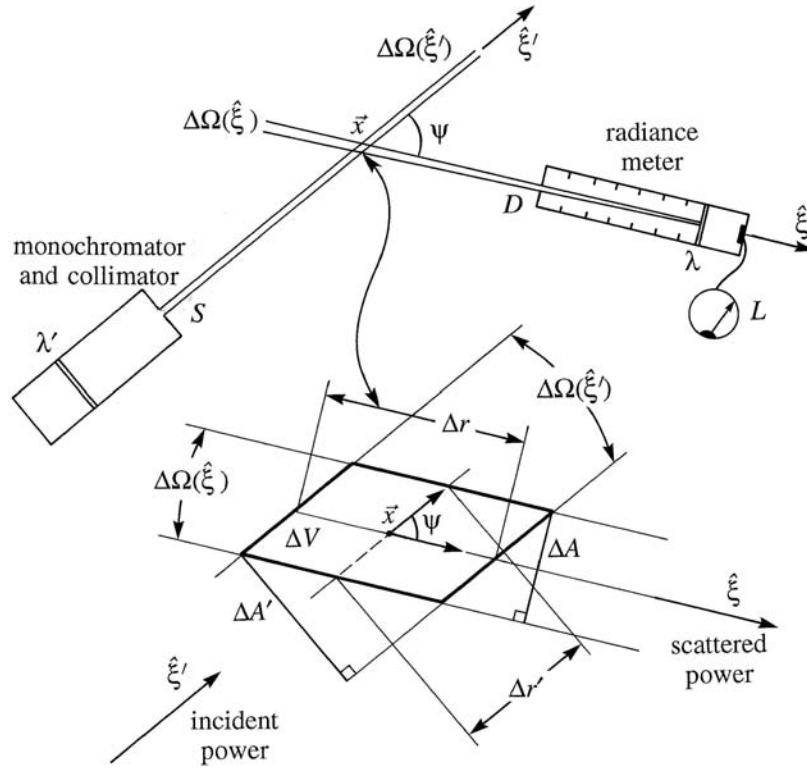
Fig. 5.1. Geometry used in defining elastic and inelastic volume scattering functions. [redrawn from Preisendorfer (1987)]

the narrow field of view of $\vec{x}$ as seen from D define an element of volume ΔV in the medium about $\vec{x}$, as shown in the inset of Fig. 5.1. This plan view of the volume is shown as a parallelogram with dimensions as depicted in the inset. It is assumed that the volume ΔV is small enough that only single scattering takes place within ΔV, although the photons in ΔV are scattered throughout the volume. Those scattered photons that go off toward point D produce an observed spectral radiance $L_{\Delta r}(\vec{x};\hat{\xi};\lambda)$ at point $\vec{x}$, in direction $\hat{\xi}$, of wavelength λ, as measured by the instrument at point D. The subscript Δr reminds us that this *path radiance is generated* within the short path of length Δr (in meters) in ΔV along direction $\hat{\xi}$. Thus the *spectral radiance generated per unit distance along direction $\hat{\xi}$* is given by

$$L_*^{\mathrm{E}}(\vec{x};\hat{\xi};\lambda) \equiv \frac{L_{\Delta r}(\vec{x};\hat{\xi};\lambda)}{\Delta r} \qquad (\mathrm{W}\ \mathrm{m}^{-3}\ \mathrm{sr}^{-1}\ \mathrm{nm}^{-1}). \qquad (5.1)$$

L_*^{E} is called the *path function for elastic scattering*.

The photons of wavelength $\lambda'(=\lambda)$ from point S giving rise to this path radiance generate unpolarized irradiance of some magnitude $E_{\mathrm{i}}(\vec{x};\hat{\xi}';\lambda)$ over the projected face of ΔV, normal to $\hat{\xi}'$, and of area $\Delta A'$, as shown in Fig. 5.1. We may reasonably expect that the radiance $L_{\Delta r}$ generated per unit path length in volume ΔV is directly proportional to the incident spectral irradiance E_{i} falling on ΔV. Denoting the proportionality constant by $\beta(\vec{x};\hat{\xi}'{\rightarrow}\hat{\xi}\ ;\lambda)$, we can write

$$\beta(\vec{x};\hat{\xi}'{\rightarrow}\hat{\xi};\lambda) \equiv \frac{L_{\Delta r}(\vec{x};\hat{\xi};\lambda)/\Delta r}{E_{\mathrm{i}}(\vec{x};\hat{\xi}';\lambda)} \qquad (\mathrm{m}^{-1}\ \mathrm{sr}^{-1}). \qquad (5.2)$$

The path radiance can be written in terms of the spectral intensity $I_{\Delta r}$ generated along path Δr as [recall Eqs. (1.20) and (1.29)]

$$L_{\Delta r} = \frac{I_{\Delta r}}{\Delta A},$$

where ΔA is the projected area of volume ΔV normal to $\hat{\xi}$, as shown in Fig. 5.1. Using this equation in Eq. (5.2) and noting that $\Delta V = \Delta A \Delta r$ gives

$$\beta(\vec{x};\hat{\xi}'{\rightarrow}\hat{\xi};\lambda) = \frac{I_{\Delta r}(\vec{x};\hat{\xi};\lambda)}{E_{\mathrm{i}}(\vec{x};\hat{\xi}';\lambda)\ \Delta V}, \qquad (5.3)$$

which is precisely the definition of the spectral volume scattering function $\beta(\psi,\lambda)$, as was given in Eq. (3.4). Thus we have in Eq. (5.2) *yet another interpretation of the VSF as being the ratio of the radiance generated per unit path length in direction $\hat{\xi}$ to the irradiance incident on the path in direction $\hat{\xi}'$*. Recall that $\psi = \cos^{-1}(\hat{\xi}'{\cdot}\hat{\xi})$.

We can write the incident irradiance E_{i} in terms of the incident radiance as

$$E_{\mathrm{i}}(\vec{x};\hat{\xi}';\lambda) = L(\vec{x};\hat{\xi}';\lambda)\ \Delta\Omega(\hat{\xi}'),$$

where $\Delta\Omega(\hat{\xi}')$ is the solid angle along $\hat{\xi}'$, as shown in Fig. 5.1. Using this result in the denominator of Eq. (5.2), and using Eq. (5.1) in the numerator, gives

$$\begin{aligned} L_*^{\mathrm{E}}(\vec{x};\hat{\xi};\lambda) &= L(\vec{x};\hat{\xi}';\lambda)\ \beta(\vec{x};\hat{\xi}'{\rightarrow}\hat{\xi};\lambda)\ \Delta\Omega(\hat{\xi}') \\ &= L(\vec{x};\hat{\xi}';\lambda)\ \beta(\vec{x};\psi;\lambda)\ \Delta\Omega(\hat{\xi}'). \end{aligned} \qquad (5.4)$$

This equation relates the path function to the incident radiance and the volume scattering function.

We have considered only one incident direction $\hat{\xi}'$ in the development of Eq. (5.4). In general, in a natural water body, photons will be passing through point $\vec{x}$ in all directions $\hat{\xi}'$ in Ξ, and each of these beams will make a contribution to the path function for direction $\hat{\xi}$. We can sum up all of these contributions to L_*^E by replacing the right hand side of Eq. (5.4) by an integral over all $\hat{\xi}'$:

$$L_*^E(\vec{x};\hat{\xi};\lambda) = \int_{\hat{\xi}'\epsilon\Xi} L(\vec{x};\hat{\xi}';\lambda)\,\beta(\vec{x};\hat{\xi}'\to\hat{\xi};\lambda)\,d\Omega(\hat{\xi}')$$

$$(\text{W m}^{-3}\text{ sr}^{-1}\text{ nm}^{-1}).$$

(5.5)

This equation shows how much radiance is gained per unit distance along a collimated beam in direction $\hat{\xi}$, owing to elastic scattering into direction $\hat{\xi}$ of photons arriving at point $\vec{x}$ and traveling in all directions $\hat{\xi}'$. The subscript "*" reminds us that L_*^E is a path function, i.e. a radiance generated per unit distance, and the superscript "E" reminds us that L_*^E is for elastic scattering only. Equation (5.5) is the desired quantitative description of radiative process (iv).

Symmetries of the volume scattering function

We shall use the notations $\beta(\hat{\xi}'\to\hat{\xi})$ and $\beta(\psi)$ interchangeably, depending on whether we wish to emphasize the incident and scattered directions, $\hat{\xi}' = (\theta',\phi') = (\mu',\phi')$ and $\hat{\xi} = (\theta,\phi) = (\mu,\phi)$ respectively, or the angle ψ between the directions. We often drop the position $\vec{x}$ and wavelength λ arguments as understood. Equation (1.11) gives the connections between the directions and the scattering angle:

$$\cos\psi = \hat{\xi}'\cdot\hat{\xi}$$
$$= \mu'\mu + \sqrt{1-\mu'^2}\sqrt{1-\mu^2}\cos(\phi'-\phi)$$
$$= \cos\theta'\cos\theta + \sin\theta'\sin\theta\cos(\phi'-\phi).$$

(5.6)

We already have seen in Chapter 3 that VSF's for natural waters depend only on ψ, and not upon the individual directions $\hat{\xi}'$ and $\hat{\xi}$ themselves. The VSF's are usually highly peaked in the forward direction; recall Figs. 3.11-3.14. In hydrologic optics this situation is usually called *anisotropic scattering*, even though the *medium* (e.g. sea water) responsible for the scattering is directionally *isotropic*. This apparent mismatch of terms

– anisotropic scattering occurring in isotropic media – makes sense if the meaning of isotropic (the same in all directions) is kept in mind. The amount of scattering is different for different $\hat{\xi}$ directions (for a given incident direction $\hat{\xi}'$), even though the optical properties of the water are the same in all directions.   The term *isotropic scattering* refers to the situation of $\beta(\psi)$ being *independent of* ψ, although *this situation never occurs in nature.* The closest approximation to isotropic scattering in nature is Rayleigh scattering, as seen in Eq. (3.29). *Anisotropic media*, i.e. media whose optical properties depend on the direction a photon is traveling within the medium, have VSF's that depend on $\hat{\xi}'$ and $\hat{\xi}$ individually, and not on just $\hat{\xi}'\cdot\hat{\xi}$. Such scattering is also termed "anisotropic," although the scattering process is clearly more complicated than that in seawater.   Table 5.1 organizes this somewhat confusing terminology.

Equation (5.6) yields several useful symmetry relations for natural-water VSF's, $\beta(\hat{\xi}'{\to}\hat{\xi}) = \beta(\mu',\phi'{\to}\mu,\phi) = \beta(\psi)$:

(i)   Invariance under interchange of μ' and μ:

$$\beta(\mu',\phi'{\to}\mu,\phi) = \beta(\mu,\phi'{\to}\mu',\phi), \qquad (5.7a)$$

(ii)   Invariance under interchange of ϕ' and ϕ:

$$\beta(\mu',\phi'{\to}\mu,\phi) = \beta(\mu',\phi{\to}\mu,\phi'), \qquad (5.7b)$$

(iii)   Invariance under simultaneous sign changes of μ' and μ:

$$\beta(\mu',\phi'{\to}\mu,\phi) = \beta(-\mu',\phi'{\to}-\mu,\phi), \qquad (5.7c)$$

(iv)   Invariance under simultaneous shifts of ϕ' and ϕ:

$$\beta(\mu',\phi'{\to}\mu,\phi) = \beta(\mu',\phi'+\phi_o{\to}\mu,\phi+\phi_o). \qquad (5.7d)$$

(v)   As a special case of property (iv), set $\phi_o = -\phi'$. Then with the help of (ii),

$$\beta(\mu',\phi'{\to}\mu,\phi) = \beta(\mu',0{\to}\mu,\phi-\phi') = \beta(\mu',0{\to}\mu,-(\phi-\phi')).$$
$$(5.7e)$$

Equation (5.7e) shows that $\beta(\mu',\phi'{\to}\mu,\phi)$ is an even function of $\phi - \phi'$. This observation, in combination with the other symmetry relations of Eq. (5.7), will lead to significant reductions in the computations necessary to solve the RTE, as we shall see in Chapter 8.

Table 5.1. Terminology used to classify the directional symmetries of
scattering processes and scattering media.

scattering process	scattering medium	example
isotropic scattering: $\beta(\hat{\xi}' \to \hat{\xi}) = \beta(\psi)$ is independent of ψ	does not occur in nature	—
"symmetric" anisotropic scattering: $\beta(\hat{\xi}' \to \hat{\xi}) = \beta(\hat{\xi}' \cdot \hat{\xi}) = \beta(\psi)$ depends only on ψ and is symmetric about $\psi = 90°$	*isotropic medium:* e.g. randomly spaced and randomly oriented very small ($\ll \lambda$) particles	Rayleigh or Raman scattering by water molecules
"asymmetric" anisotropic scattering: $\beta(\hat{\xi}' \to \hat{\xi}) = \beta(\hat{\xi}' \cdot \hat{\xi}) = \beta(\psi)$ depends only on ψ	*isotropic medium:* e.g. randomly spaced and randomly oriented large ($> \lambda$) particles	scattering by phytoplankton suspended in water
"completely" anisotropic scattering: $\beta(\hat{\xi}' \to \hat{\xi})$ depends on $\hat{\xi}'$ and $\hat{\xi}$ individually	*anisotropic medium:* e.g. particles arranged on a regular lattice	scattering by a crystal
	e.g. randomly spaced asymmetric particles that are oriented in direction	scattering by cirrus clouds or ice fogs in calm air

The scattering coefficient for elastic scattering

In deriving the path function, we held the direction $\hat{\xi}$ of the scattered beam fixed, and integrated over all incident directions $\hat{\xi}'$. The reverse of this operation is to hold the incident direction $\hat{\xi}'$ fixed, and integrate over all scattered directions $\hat{\xi}$. Integrating the VSF over all $\hat{\xi}$ gives

$$b(\vec{x};\hat{\xi}';\lambda) \equiv \int_{\hat{\xi} \in \Xi} \beta(\vec{x};\hat{\xi}' \to \hat{\xi};\lambda)\, d\Omega(\hat{\xi}) \qquad (\text{m}^{-1}) .$$

(5.8)

This equation gives all of the elastic scattering *losses* from an incident beam in direction $\hat{\xi}'$. In isotropic media such as natural waters, $b(\vec{x};\hat{\xi}';\lambda)$ is independent of $\hat{\xi}'$. In other words, $b(\vec{x};\hat{\xi}';\lambda)$ is just the spectral scattering coefficient

$$b(\vec{x};\lambda) \;=\; \int_{\Xi} \beta(\vec{x};\psi;\lambda)\, d\Omega \;=\; 2\pi \int_0^{\pi} \beta(\vec{x};\psi;\lambda)\, \sin\psi\, d\psi\;,$$

as was defined in Eq. (3.5).

n Chapter 3 we saw specific forms for elastic scattering functions, e.g. Eq. (3.28) for pure water, and Table 3.10 for sea water.

5.3 Inelastic Scattering

We now return to the setting of Fig. 5.1 and consider the possibility that the wavelength λ of the scattered light is different from the wavelength λ' of the incident light. We suppose that the light source at *S* is emitting radiant power over a narrow range of wavelengths $\Delta\lambda'$ centered on λ', and that the detector at *D* is sensitive only to wavelength λ, which is not in $\Delta\lambda'$. In analogy to Eq. (5.2), we define the *spectral volume inelastic scattering function* as the ratio of spectral radiance generated in direction $\hat{\xi}$ at wavelength λ, per unit distance and unit incident wavelength, to the irradiance incident on the path in direction $\hat{\xi}'$ at wavelength $\lambda' \neq \lambda$:

$$\beta^{\mathrm{I}}(\vec{x};\hat{\xi}'{\to}\hat{\xi};\lambda'{\to}\lambda) \;=\; \frac{L_{\Delta r}(\vec{x};\hat{\xi};\lambda)/(\Delta r\,\Delta\lambda')}{E_{\mathrm{i}}(\vec{x};\hat{\xi}';\lambda')}$$

$$\equiv \frac{L_*^{\mathrm{I}}(\vec{x};\hat{\xi};\lambda)}{L(\vec{x};\hat{\xi}';\lambda')\,\Delta\Omega'\,\Delta\lambda'} \quad (\mathrm{m}^{-1}\ \mathrm{sr}^{-1}\ \mathrm{nm}^{-1})\,. \qquad (5.9)$$

Here we have defined the inelastic path function L_*^{I} in analogy with Eq. (5.1). The superscript "I" on L_*^{I} and β^{I} reminds us that these quantities refer to inelastic scattering only. Note that Eq. (5.9) can be rewritten as

$$\beta^{\mathrm{I}}(\vec{x};\hat{\xi}'{\to}\hat{\xi};\lambda'{\to}\lambda) \;=\; \frac{I_{\Delta r}(\vec{x};\hat{\xi};\lambda)}{E_{\mathrm{i}}(\vec{x};\hat{\xi}';\lambda')\,\Delta\lambda'\,\Delta V}\;,$$

which is the inelastic counterpart to Eqs. (3.4) and (5.3).

The inelastic counterpart to Eq. (5.5),

$$L_*^{\mathrm{I}}(\vec{x};\hat{\xi};\lambda) \;=\; \int\limits_{\Xi}\int\limits_{\Lambda} L(\vec{x};\hat{\xi}';\lambda')\,\beta^{\mathrm{I}}(\vec{x};\hat{\xi}'\to\hat{\xi};\lambda'\to\lambda)\,d\lambda'\,d\Omega(\hat{\xi}')$$

$$(5.10)$$

$$(\mathrm{W\ m^{-3}\ sr^{-1}\ nm^{-1}}),$$

shows how much radiance of wavelength λ is gained per unit distance along direction $\hat{\xi}$, owing to inelastic scattering into direction $\hat{\xi}$ and wavelength λ by photons of all other wavelengths λ', which are traveling in all directions $\hat{\xi}'$. In Eq. (5.10), Λ denotes the entire electromagnetic spectrum. Thus the λ' integration is over all wavelengths: $0 \le \lambda' < \infty$. In practice, β^{I} is nonzero only for some small subset of Λ, e.g. the near-UV to near-IR region. Moreover, the λ' integration in Eq. (5.10) is well defined even though β^{I} is defined in Eq. (5.9) only for $\lambda' \ne \lambda$. By a basic property of Riemann integrals, we can assign any value to β^{I} when $\lambda' = \lambda$ without affecting the value of the integral. For convenience, we set $\beta^{\mathrm{I}} = 0$ when $\lambda' = \lambda$, i.e.

$$\beta^{\mathrm{I}}(\vec{x};\hat{\xi}'\to\hat{\xi};\lambda\to\lambda) \;\equiv\; 0$$

for all λ. Equation (5.10) is the quantitative description of radiative process (v).

The *volume inelastic scattering coefficient* [see Supplementary Note 8] is defined by

$$b^{\,\mathrm{I}}(\vec{x};\hat{\xi}';\lambda'\to\lambda) \;\equiv\; \int\limits_{\Xi} \beta^{\mathrm{I}}(\vec{x};\hat{\xi}'\to\hat{\xi};\lambda'\to\lambda)\,d\Omega(\hat{\xi}) \quad (\mathrm{m^{-1}\ nm^{-1}}),$$

$$(5.11)$$

in analogy to Eq. (5.8). In natural waters, b^{I} is independent of $\hat{\xi}'$ and we can write just $b^{\mathrm{I}}(\vec{x};\lambda'\to\lambda)$.

Definition (5.11) allows us to define the *volume inelastic scattering phase function*, $\widetilde{\beta}^{\,\mathrm{I}}$, as

$$\widetilde{\beta}^{\,\mathrm{I}}(\vec{x};\hat{\xi}'\to\hat{\xi};\lambda'\to\lambda) \;\equiv\; \frac{\beta^{\mathrm{I}}(\vec{x};\hat{\xi}'\to\hat{\xi};\lambda'\to\lambda)}{b^{\,\mathrm{I}}(\vec{x};\lambda'\to\lambda)} \qquad (\mathrm{sr^{-1}}).$$

$$(5.12)$$

This equation is analogous to Eq. (3.7). The inelastic scattering phase function $\widetilde{\beta}^{\,\mathrm{I}}$ satisfies the same normalization condition (3.8), namely

$$2\pi \int\limits_{0}^{\pi} \widetilde{\beta}^{\,\mathrm{I}}(\psi)\,\sin\psi\,d\psi \;=\; 1,$$

as does the elastic scattering phase function $\widetilde{\beta}$.

Two inelastic processes that are important in natural waters are Raman scattering by water molecules and fluorescence by phytoplankton

pigments and dissolved organic material. We shall postpone a discussion of these processes until Sections 5.14 and 5.15, respectively, at which time we shall see the specific forms of β^I, b^I, and $\tilde{\beta}^I$ necessary for the description of those processes.

5.4 True, Inelastic, and Total Absorption Coefficients

The introduction of the volume absorption coefficient into radiative transfer theory requires care in order to accurately account for the particular fate of an absorbed photon. There are two distinct cases of "absorption-like" activity to consider when a photon of wavelength λ' in the incident beam of Fig. 5.1 arrives in the volume ΔV surrounding point $\vec{x}$. In the first case, the photon is truly absorbed and its energy is converted into nonradiant energy. This process is called *true absorption.* In the second case, the photon's energy momentarily raises the internal energy of the absorbing atom or molecule, and then a photon of generally (but not always) longer wavelength λ is emitted. This process is called *inelastic*, or *transpectral*, *absorption* because, as far as the incident radiant power of wavelength λ' is concerned, there is a loss or an "absorption" of radiant power from *that* wavelength.

We shall denote the *true absorption coefficient* by $a^e(\vec{x};\lambda')$, with units of m^{-1}. The superscript "e" reminds us that this absorption results in *extinction* of radiant energy. The inelastic absorption coefficient $a^I(\vec{x};\lambda')$ is defined by

$$a^I(\vec{x};\lambda') \equiv \int_\Lambda b^I(\vec{x};\lambda' \to \lambda)\, d\lambda \qquad (m^{-1}).$$

(5.13)

It should be clear from our previous discussions that Eq. (5.13) accounts for energy lost (scattered) to all wavelengths other than the incident wavelength λ'. The *total absorption coefficient* $a(\vec{x};\lambda')$ is defined by

$$a(\vec{x};\lambda') \equiv a^e(\vec{x};\lambda') + a^I(\vec{x};\lambda') \qquad (m^{-1}).$$

(5.14)

Clearly, if there is no inelastic scattering, $a = a^e$ is the spectral absorption coefficient as defined in Eq. (3.1).

Recent literature shows no uniformity of notation or terminology for the quantities b^I and a^I just defined. We call b^I the inelastic *scattering* coefficient to emphasize that it is a measure of how strongly light changes

direction, i.e. is scattered, in the common connotation of the term . We call a^I the inelastic *absorption* coefficient because it measures how strongly light disappears from wavelength λ', just as does the true absorption coefficient a^e.

5.5 Total Attenuation

We can now account for all of the possible losses of radiant power from a collimated beam of photons. Consider a beam of radiance $L(\vec{x};\hat{\xi};\lambda)$. As the photons travel from point $\vec{x}$ to point $\vec{x} + \Delta\vec{x}$, a distance $\Delta r = |\Delta\vec{x}|$ away in the $\hat{\xi}$ direction, some of them will be lost via true absorption, [process (iii)], some will be changed to other wavelengths [inelastic absorption, process (ii)], and some will be scattered to other directions [elastic scattering, process (i)]. The decrease in radiance when going from $\vec{x}$ to $\vec{x} + |\Delta\vec{x}|$ is proportional to the distance and to the radiance. Thus for small Δr, the radiance $L(\vec{x}+\Delta\vec{x};\hat{\xi};\lambda)$ at $\vec{x} + \Delta\vec{x}$ is given by

$$L(\vec{x} + \Delta\vec{x};\hat{\xi};\lambda) = L(\vec{x};\hat{\xi};\lambda) - \left[a^e(\vec{x};\lambda) + a^I(\vec{x};\lambda) + b(\vec{x};\lambda) \right] \Delta r\, L(\vec{x};\hat{\xi};\lambda).$$

Upon letting $\Delta L(\vec{x}) = L(\vec{x}+\Delta\vec{x}) - L(\vec{x})$, we get

$$
\begin{aligned}
\frac{\Delta L(\vec{x};\hat{\xi};\lambda)}{\Delta r} &= -\left[a^e(\vec{x};\lambda) + a^I(\vec{x};\lambda) + b(\vec{x};\lambda) \right] L(\vec{x};\hat{\xi};\lambda) \\
&\equiv -c(\vec{x};\lambda)\, L(\vec{x};\hat{\xi};\lambda).
\end{aligned}
\tag{5.15}
$$

Here we have defined the *total beam attenuation coefficient $c(\vec{x};\lambda)$* as

$$
\begin{aligned}
c(\vec{x};\lambda) &\equiv a^e(\vec{x};\lambda) + a^I(\vec{x};\lambda) + b(\vec{x};\lambda) \\
&= a(\vec{x};\lambda) + b(\vec{x};\lambda),
\end{aligned}
\tag{5.16}
$$

which corresponds to Eq. (3.3). Equation (5.15) expresses the important result that *all of the radiative loss processes can be accounted for in the single measurement of beam attenuation at the wavelength of interest.*

5.6 True Emission

The only radiative process not yet discussed is number (vi), the creation of radiance by conversion of nonradiant energy into light. This process is called *true emission* to distinguish it from the apparent emission

of radiance at wavelength λ owing to inelastic scatter from wavelengths $\lambda' \neq \lambda$.

The mathematical description of true emission is given in terms of a source path function $L_*^S(\vec{x};\hat{\xi};\lambda)$, with units of radiance per unit length, that specifies how much radiance of wavelength λ is created at location $\vec{x}$ per unit distance along direction $\hat{\xi}$. The source path function L_*^S is clearly analogous in nature to the path functions discussed above. The functional form of L_*^S must be tailored to describe the particular emission process at hand, e.g. bioluminescence or an underwater artificial light source. In many instances of oceanographic interest, L_*^S can be modeled as

$$L_*^S(\vec{x};\hat{\xi};\lambda) = S_o(\vec{x};\lambda)\,\tilde{\beta}^S(\hat{\xi})\,.$$

Here S_o, with units of $W\,m^{-3}\,nm^{-1}$, gives the spectral radiant power emitted at $\vec{x}$ and λ; and $\tilde{\beta}^S(\hat{\xi})$, with units of sr^{-1}, give the directional distribution of the emitted light.

As a simple example of L_*^S, consider a uniform distribution of bioluminescent organisms emitting spectral radiant power of magnitude $S_o(\lambda)$ $W\,m^{-3}\,nm^{-1}$. If this power is emitted isotropically into all directions (i.e. into 4π sr), then we have

$$L_*^S(\vec{x};\hat{\xi};\lambda) = \frac{S_o(\lambda)}{4\pi} \qquad (W\,m^{-3}\,sr^{-1}\,nm^{-1})\,.$$

Bioluminescence can be a significant source of light in the oceans, and we shall return to this topic in Section 5.16.

In atmospheric optics at infrared wavelengths, and in astrophysical optics at visible wavelengths, blackbody emission by the medium itself is a significant internal source of radiant energy. In such situations, L_b of Eq. (2.2) can be used to construct the source path function. At the temperatures of liquid water there is essentially no thermal emission at visible wavelengths, and therefore blackbody radiation is unimportant in hydrologic optics.

5.7 Radiance Transfer Equations

The discussion of Section 4.2 leading to the n^2 law for radiance, Eq. (4.21), and to the fundamental theorem of radiometry, Eq. (4.22), showed that the radiance along a path can change owing to purely geometric effects induced by changes in the real index of refraction n along the path. We learned that, in the absence of absorption and scattering, the quantity L/n^2,

which is sometimes called the reduced radiance, remains invariant along a path.

In Section 4.2 our interest was on the large change in the index of refraction at the air-water surface. As we learned in Section 3.8, the index of refraction within a water body changes from point to point for a variety of reasons. Changes in *n* on scales from molecular size to ~1 cm are caused by random molecular motions, by organic or inorganic particulate matter, and by turbulent fluctuations in temperature and salinity. Such changes already have been accounted for in the volume scattering functions for pure water and for particles.   For most oceanographic purposes, only these small-scale fluctuations in *n* are significant, and *n* can be taken as constant. However, *n* sometimes fluctuates over long path lengths (centimeters to meters) owing to large-scale changes in water temperature and salinity. Such changes in *n* can change the radiance along a path by causing slight changes in the direction $\hat{\xi}$ of ray propagation.

We can allow for any changes in *n*, in addition to those parameterized in the volume scattering functions, simply by taking L/n^2 as the quantity of interest along a path. In particular, any occurrence of *L* in our previous development can be replaced by L/n^2. For example, the path function for elastic scattering, Eq. (5.5), becomes

$$\mathcal{L}_*^{\mathrm{E}}(\vec{x};t;\hat{\xi};\lambda) \equiv \int_{\hat{\xi}' \in \Xi} \left(\frac{L(\vec{x};t;\hat{\xi}';\lambda)}{n^2(\vec{x};t;\lambda)} \right) \beta(\vec{x};t;\hat{\xi}' \rightarrow \hat{\xi};\lambda) \, d\Omega(\hat{\xi}') . \qquad (5.17)$$

We have explicitly shown the time argument in Eq. (5.17) to emphasize that all quantities, including *n*, may change with time. Changes in L/n^2 along a path can be attributed to the various absorption and scattering processes occurring along the path.

We are now nearly in position to derive the equation governing the change in L/n^2 as we move along a path in direction $\hat{\xi}$. As in Eq. (5.15), we think of moving from point $\vec{x}$ to point $\vec{x} + \Delta\vec{x}$, and of taking the limit as $\Delta r = |\Delta\vec{x}| \rightarrow 0$. Notationally, we let

$$\lim_{\Delta r \rightarrow 0} \frac{\Delta(L/n^2)}{\Delta r} \equiv \frac{D(L/n^2)}{Dr} ,$$

where *D/Dr* denotes the total rate of change along the path. The total rate of change can be expressed in terms of the usual substantive derivative by noting that

$$\frac{D}{Dr} = \frac{1}{v} \frac{D}{Dt} ,$$

where $v = v(\vec{x};t;\lambda)$ is the speed of light *in the medium* at position $\vec{x}$, at time

t, for wavelength λ. The speed v can be written as $v(\vec{x};t;\lambda) = c/n(\vec{x};t;\lambda)$, where $c = 2.998\times10^8$ m s^{-1} is the speed of light *in vacuo* and n is the index of refraction. Finally, we recall the meaning of the substantive derivative:

$$\frac{D}{Dt} \equiv \frac{\partial}{\partial t} + \vec{v}{\cdot}\nabla \, ,$$

where

$$\nabla = \hat{i}_1 \frac{\partial}{\partial x_1} + \hat{i}_2 \frac{\partial}{\partial x_2} + \hat{i}_3 \frac{\partial}{\partial x_3}$$

is the gradient operator expressed in the coordinate system of Fig. 4.2. Thus

$$\frac{D}{Dr} = \frac{1}{v}\frac{D}{Dt} = \frac{1}{v}\frac{\partial}{\partial t} + \hat{\xi}{\cdot}\nabla \, , \tag{5.18}$$

since the photons are traveling with speed v in direction $\hat{\xi} = \vec{v}/v$.

The general RTE

We can now equate the general *mathematical* expression for the change in L/n^2 along a path with the sum of the *physical* terms causing that change. The result is

$$\frac{1}{v}\frac{\partial}{\partial t}\left(\frac{L}{n^2}\right) + \hat{\xi}{\cdot}\nabla\left(\frac{L}{n^2}\right) = -c\left(\frac{L}{n^2}\right) + \mathscr{L}_*^{\mathrm{E}} + \mathscr{L}_*^{\mathrm{I}} + \mathscr{L}_*^{\mathrm{S}}$$
$$(\mathrm{W \ m}^{-3} \ \mathrm{sr}^{-1} \ \mathrm{nm}^{-1}) \, . \tag{5.19}$$

The script letters for the path functions and the source term indicate the incorporation of the n^{-2} factors on L, as in Eq. (5.17). Note that c in Eq. (5.19) is the beam attenuation coefficient, not the speed of light.

Equation (5.19) *is the most general form of the radiance transfer equation for unpolarized radiance.* It governs the time-dependent, three-dimensional behavior of the radiance $L(\vec{x};t;\hat{\xi};\lambda)$, including the effects of inelastic scattering and internal sources. It is also valid for anisotropic media, if we take the inherent optical properties to be functions of direction, e.g. $n = n(\vec{x};t;\hat{\xi};\lambda)$, and $b = b(\vec{x};t;\hat{\xi};\lambda)$, as in Eq. (5.8). The equation is easily elevated to the case of polarized radiance; this is done in Section 5.12.

We present Eq. (5.19) for completeness. However, our primary interest in this book is in time-independent radiative transfer in horizontally homogeneous water bodies with a constant index of refraction. In this case, the constant n^{-2} factor divides out on both sides of Eq. (5.19),

$$\frac{\partial L}{\partial t} = 0,$$

and

$$\hat{\xi} \cdot \nabla L = \xi_3 \frac{\partial L}{\partial x_3} = \mu \frac{dL}{dz}.$$

In the last equation, we have recalled our convention (from Section 4.1) of letting $z = x_3$ denote the geometric depth in meters, and that $\xi_3 = \cos\theta = \mu$ [Eq. (1.9)]. Since only one spatial variable, z, remains, we have changed the partial derivative to an ordinary derivative. The RTE is now

$$\frac{dL}{dr} = \mu \frac{dL}{dz} = -cL + L_*^{\mathbf{E}} + L_*^{\mathbf{I}} + L_*^{\mathbf{S}}. \tag{5.20}$$

Note that the increment of path length $dr = dz/\mu$ is always positive. Photons heading downward ($0 \le \theta \le \pi/2$, so that $\mu \ge 0$) are traveling in the positive z direction; hence $dz \ge 0$, $\mu \ge 0$, and $dr \ge 0$. Photons heading upward ($\pi/2 < \theta \le \pi$, so that $\mu < 0$) are traveling in the negative z direction; hence $dz < 0$, $\mu < 0$, and $dr > 0$. The change dL along a path segment dr can be positive or negative, depending on the relative sizes of the terms on the right hand side of Eq. (5.20).

Equation (5.20) still contains radiances of all wavelengths, by virtue of the $L_*^{\mathbf{I}}$ term defined in Eq. (5.10). Solution of (5.20) thus implies a *simultaneous* solution for L at *all* wavelengths; only the true emission term $L_*^{\mathbf{S}}$ is considered known.

The monochromatic RTE for plane-parallel waters

It is common practice in hydrologic optics to combine the inelastic scatter and true emission terms into an *effective source function S*:

$$S \equiv L_*^{\mathbf{I}} + L_*^{\mathbf{S}}. \tag{5.21}$$

The RTE (5.20) then becomes

$$\mu \frac{dL}{dz} = -cL + L_*^{\mathbf{E}} + S. \tag{5.22}$$

Equation (5.22), although completely equivalent to Eq. (5.20), is *viewed* as an equation for *monochromatic* radiance of wavelength λ. *The effective source term S is considered known*, even though it may include a contribution to wavelength λ by inelastic scattering from other wavelengths $\lambda' \neq \lambda$. Solution of Eq. (5.22) thus implies a solution at only one wavelength. If L is desired at many wavelengths, with proper accounting

for inelastic scattering, then we must first solve Eq. (5.22) at some wavelength λ_1, for which there is *no* contribution *from* other wavelengths. If $L(z;\hat{\boldsymbol{\xi}};\lambda_1)$ inelasticly contributes *to* wavelength λ_2, then the source term $S(z;\hat{\boldsymbol{\xi}};\lambda_2)$ can be computed from the solution $L(z;\hat{\boldsymbol{\xi}};\lambda_1)$, and we can proceed with the solution of Eq. (5.22) for λ_2. This process can be repeated, iterating between wavelengths if necessary, until we have obtained solutions at all desired wavelengths. Thus the philosophically different viewpoints for Eqs. (5.20) and (5.22) determine whether we use one simultaneous, multi-wavelength solution technique, or a sequence of single-wavelength solution techniques.

Standard form of the RTE

Equation (5.22) is written in terms of the geometric depth z and the volume scattering function β. Written out in full, the monochromatic RTE is

$$
\mu \frac{dL(z;\hat{\xi};\lambda)}{dz} = -c(z;\lambda)\, L(z;\hat{\xi};\lambda)
$$
$$
+ \int_{\Xi} L(z;\hat{\xi}';\lambda)\, \beta(z;\hat{\xi}'\!\to\!\hat{\xi};\lambda)\, d\Omega(\hat{\xi}') \;+\; S(z;\hat{\xi};\lambda) \qquad (5.23)
$$
$$
(\text{W m}^{-3}\,\text{sr}^{-1}\,\text{nm}^{-1})\,.
$$

The corresponding equation written in terms of the dimensionless optical depth ζ is obtained by dividing Eq. (5.23) by $c(z;\lambda)$ and recalling definition (4.1) for optical depth: $d\zeta = c(z)dz$. In addition, let us write the VSF β as the product of the scattering coefficient b and the phase function $\tilde{\beta}$, as in Eq. (3.7). Recalling definition (3.9) for the single-scattering albedo, $\omega_o = b/c$, then gives

$$
\mu \frac{dL(\zeta;\hat{\xi};\lambda)}{d\zeta} = -L(\zeta;\hat{\xi};\lambda) \;+\; \omega_o(\zeta;\lambda) \int_{\Xi} L(\zeta;\hat{\xi}';\lambda)\, \tilde{\beta}(\zeta;\hat{\xi}'\!\to\!\hat{\xi};\lambda)\, d\Omega(\hat{\xi}')
$$
$$
(5.24)
$$
$$
+ \frac{1}{c(\zeta;\lambda)} S(\zeta;\hat{\xi};\lambda) \qquad (\text{W m}^{-2}\,\text{sr}^{-1}\,\text{nm}^{-1})\,.
$$

We now show all quantities as a function of optical depth. Form (5.24) of the RTE yields an important observation: *Any two water bodies having the same single-scattering albedo ω_o, phase function $\tilde{\beta}$, beam attenuation coefficient c, and source function S (and the same boundary conditions, including incident radiances) will have the same radiance distribution L. In source-free waters, ω_o, $\tilde{\beta}$, and the boundary conditions are sufficient to determine the radiance distribution as a function of optical depth. If we*

wish to convert the optical-depth solution to geometric depth, then c is also required. It is customary in radiative transfer theory to specify the medium in terms of ω_o, c, and $\tilde{\beta}$, and to use optical depth ζ as the spatial variable. In oceanographic work, one most often measures or models a, c and β as functions of geometric depth z. Conversion between (a, c, β, z) and $(\omega_o, c, \tilde{\beta}, \zeta)$ is easily made using the appropriate equations seen previously.

The integrodifferential Eq. (5.24), or its equivalent (5.23), is the form of the RTE with which we shall work in the remainder of this book. We shall expend great effort in learning how to solve this equation for inherent optical properties, source functions, and boundary conditions that are realistic approximations of those found in natural water bodies. We shall study selected numerical solutions of Eq. (5.24) with the goal of understanding the behavior of $L(\zeta;\hat{\xi};\lambda)$ in natural waters. These matters are the subject of Parts III and IV of our book.

Limitations of the RTE

We already have commented in Section 4.1 that radiative transfer theory is a macroscopic-level, linear approximation that is valid at low irradiances and low photon energies. Even within this domain, additional requirements must be satisfied. We have implicitly assumed that the medium of interest is a continuous material, at least when viewed on the macroscopic level, so that the limits seen in Eqs. (3.1), (3.2) and (3.4) have meaning. Our treatment of scattering by particles in Sections 3.8 and 3.11 also supposed that the scattering particles were far apart (relative to λ) and randomly arranged. These conditions are well satisfied in many natural situations ranging from stellar and planetary atmospheres to the deep ocean. We therefore can employ the theory, as embodied in the RTE, to the everyday problems of hydrologic optics without further concern about its applicability. Fante (1981) has examined in detail the sufficient conditions for the validity of the RTE.

However, it is not hard to violate the assumptions implicit in our treatment of scattering if we go beyond atmospheric and oceanic media. Consider, for example, the problem of visible light traveling through a slab packed with small translucent particles, e.g. newly fallen snow, or dust particles of size ~1 μm. Now the scattering particles are no longer far apart. They are touching each other, and the electromagnetic wave scattered by one particle immediately encounters neighboring particles, which scatter it again, and so on. Even if we know the optical properties of an isolated particle, we cannot expect to obtain the IOP's of a dense collection of such particles in the simple manner of Eq. (3.52). It may still be possible to

apply the RTE to such problems, but the values to be used for the scattering and absorption properties of the medium are not easily related to the IOP's as we defined them in Sections 3.1 and 3.11.

When faced with such problems, we can in principle always return to Maxwell's equations and carry out a detailed analysis of the electromagnetic fields as they interact with the densely packed particles. This is a much more difficult problem, which is discussed, for example, in the treatise by Ishimaru (1978). In view of the general applicability of Maxwell's equations, electromagnetic theory is sometimes viewed as being more exact or more fundamental than radiative transfer theory. However, the mathematics associated with the electromagnetic-field viewpoint quickly becomes intractable when multiple scattering is present.

Because of these mathematical difficulties, we are tempted to try to reformulate the RTE in some way, so as to retain its mathematical advantages while extending its domain of validity. We are thus led to the difficult subject of *dense-medium radiative transfer*. A good introduction to this subject is the paper by Goedecke (1977).

5.8 Integral Forms of the RTE

Additional insights into radiative transfer theory can be obtained by a formal integration of Eq. (5.24). This integration leads us to the concepts of transmittance operators and global formulations of equations – concepts that will be central to our later mathematical developments.

Beer's law

For the idealized case of source-free ($S = 0$), non-scattering ($\omega_o = 0$) media, the RTE reduces to just

$$\mu \frac{dL}{d\zeta} = -L.$$

This equation is easily integrated and yields

$$L(\zeta;\hat{\xi}) = L(0;\hat{\xi}) \exp\left(-\frac{\zeta}{\mu}\right). \qquad (5.25)$$

Here $L(0;\hat{\xi})$ is the value of the radiance in direction $\hat{\xi}$ at some reference depth, which we take to be $\zeta = 0$; this *boundary value* $L(0;\hat{\xi})$ is presumed known. We have dropped the wavelength argument λ for brevity. Equation (5.25) shows that the radiance at optical depth ζ is just the radiance at $\zeta =$

0 multiplied by an exponential factor that depends on the optical depth and the direction $\mu = \cos\theta$. This result, in any of its many forms, is known as Beer's law, Bouguer's law, Lambert's law, or some hyphenated combination of these names. We shall use "Beer's law" to denote any instance of exponential attenuation of light.

Equation (5.25) certainly makes sense for the case of $\mu > 0$ (downwelling radiance). For example, radiance entering a water body at its surface decreases in magnitude with depth. But consider the case of upwelling radiance, for which $\mu < 0$. The exponential in Beer's law is then greater than one, since $\zeta > 0$ and $\mu < 0$, and $L(\zeta;\mu<0,\phi)$ *increases* with depth, which seems counterintuitive. The resolution of this paradox is easy. In the purely absorbing medium under consideration here, radiance always decreases along a path increment $dr > 0$. If the radiance at the surface, $L(0;\mu<0,\phi)$, is to have a given value, then the radiance at depth, $L(\zeta;\mu<0,\phi)$, must have a *greater* value because some photons will be absorbed in traveling upward from depth ζ to depth 0. Viewed this way, Beer's law makes sense. Note that Beer's law does *not* imply that upwelling radiance distributions increase with depth in natural water bodies. Those upwelling radiances arise because of scattering of downwelling light, a process that is neglected in Eq. (5.25).

The quantity l defined by

$$dl \equiv \frac{d\zeta}{\mu} = \frac{c(z)\,dz}{\mu}$$

is called the *optical path length* in direction μ. Note that dl is always positive, since $d\zeta > 0$ ($d\zeta < 0$) when $\mu > 0$ ($\mu < 0$). The optical depth is just the optical path length in the $\hat{\xi} = \hat{i}_3$ direction. It will be convenient to write l as

$$l = \frac{\zeta}{|\mu|} = \frac{1}{|\mu|}\int_0^z c(z')\,dz',$$

to make clear that l is always positive. For purely absorbing, source-free media we have

$$\mu\,\frac{dL}{d\zeta} = \frac{dL}{dl} = -L,$$

and Beer's law reads

$$L(l) = L(0)e^{-l},$$

which makes clear that the radiance decreases along any path of photon travel. Note that we have defined l in terms of the total beam attenuation

coefficient *c,* even though $c = a$ in the context of Beer's law.

     We can also write Beer's law as

$$L(\zeta;\hat{\xi}) = L(0;\hat{\xi}) \, T_l(\zeta;\hat{\xi}) \,, \tag{5.26}$$

if we define the *transmission function as* T_l as

$$T_l(\zeta;\hat{\xi}) \equiv e^{-l} = \exp\left[-\frac{\zeta}{|\hat{\xi}\cdot\hat{i}_3|}\right]. \tag{5.27}$$

Clearly, T_l is bounded by $0 \le T_l \le 1$. Physically, T_l is just the function that specifies what fraction of the radiance $L(0;\hat{\xi})$ is transmitted in direction $\hat{\xi}$ over an optical path length *l.* T_l plays a role within the water body that is similar to that played by the radiance transmittance functions for the air-water surface, which were first encountered in Eqs. (4.3) and (4.4). In the present situation, the constant index of refraction implies no change in a ray direction within the water body, and so T_l requires only one direction argument, $\hat{\xi}$.

Integral form of the RTE

    Let us now return to the monochromatic RTE and repeat the integration process that led to Beer's law. Multiplying both sides of Eq. (5.24) by $\mu^{-1}\exp(\zeta/\mu)$ and rearranging gives

$$\frac{d}{d\zeta}\left[L(\zeta;\hat{\xi})\exp\left(\frac{\zeta}{\mu}\right)\right] = \frac{1}{\mu}\exp\left(\frac{\zeta}{\mu}\right)\left[\frac{1}{c(\zeta)}\left(L_*^{\mathrm{E}}(\zeta;\hat{\xi}) + S(\zeta;\hat{\xi})\right)\right].$$

Integrating both sides of this equation from 0 to ζ yields

$$L(\zeta;\hat{\xi})\exp\left(\frac{\zeta}{\mu}\right) - L(0;\hat{\xi}) = \int_0^\zeta \frac{1}{\mu}\exp\left(\frac{\zeta'}{\mu}\right)\left[\frac{1}{c(\zeta')}\left(L_*^{\mathrm{E}}(\zeta';\hat{\xi}) + S(\zeta';\hat{\xi})\right)\right]d\zeta',$$

or

$$L(\zeta;\hat{\xi}) = L(0;\hat{\xi})\exp\left(-\frac{\zeta}{\mu}\right)$$

$$+ \int_0^\zeta\left[\frac{1}{\mu\,c(\zeta')}\left(L_*^{\mathrm{E}}(\zeta';\hat{\xi}) + S(\zeta';\hat{\xi})\right)\right]\exp\left(-\frac{\zeta - \zeta'}{\mu}\right)d\zeta'. \tag{5.28}$$

This equation can be expressed in term of transmission functions as

$$L(\zeta;\hat{\xi}) = L(0,\hat{\xi}) \, T_l(\zeta;\hat{\xi})$$
$$+ \int_0^\zeta \left[\frac{1}{\mu \, c(\zeta')} \left(L_*^E(\zeta';\hat{\xi}) + S(\zeta';\hat{\xi}) \right) \right] T_{l-l'}(\zeta - \zeta';\hat{\xi}) \, d\zeta' . \quad (5.29)$$

Expressed in terms of the geometric depth *z*, Eq. (5.28) reads

$$L(z;\hat{\xi}) = L(0;\hat{\xi}) \exp\left[-\frac{1}{\mu} \int_0^z c(z'') \, dz'' \right]$$
$$+ \int_0^z \left[\frac{1}{\mu} \left(L_*^E(z';\hat{\xi}) + S(z';\hat{\xi}) \right) \right] \quad (5.30)$$
$$\times \exp\left[-\frac{1}{\mu} \int_{z'}^z c(z'') \, dz'' \right] dz' .$$

Any of the Eqs. (5.28)-(5.30) is known as the *integral form of the RTE*. Since the unknown radiance $L(\zeta;\hat{\xi})$ is contained within the path function L_*^E, Eq. (5.28) brings us no closer to a solution of the RTE than does the integrodifferential equation (5.24). The integral form does however have an interesting interpretation not seen in Eq. (5.24).

Suppose an object located at depth $\zeta = 0$ is emitting radiance $L(0;\hat{\xi})$; this is the *inherent* radiance of the object. The radiance of the object when viewed at depth ζ is $L(\zeta;\hat{\xi})$; this is the *apparent* radiance of the object. The geometry of this situation is seen in Fig. 5.2, in which the object can be thought of as a point on the bottom side of the water surface. Equation (5.28) shows that the apparent radiance is composed of two parts. The first part is just the inherent radiance attenuated by the factor $T_l(\zeta;\hat{\xi}) = \exp(-l)$. The second part consists of the radiance *generated* at each depth ζ' along the path from 0 to ζ, and then attenuated by a factor $T_{l-l'}(\zeta - \zeta';\hat{\xi}) = \exp[-(l-l')]$, which is determined by the optical path length between each point of generation and the point of observation. The first part is known as the inherent, or direct beam, contribution to the apparent radiance. The second part is the path radiance, or "spacelight," contribution. Clearly, the path radiance shows how much of the observed radiance was generated along the path between the light source and the observer. Because of this interpretation, the integral form (5.28) is also known as the *apparent radiance form of the RTE*.
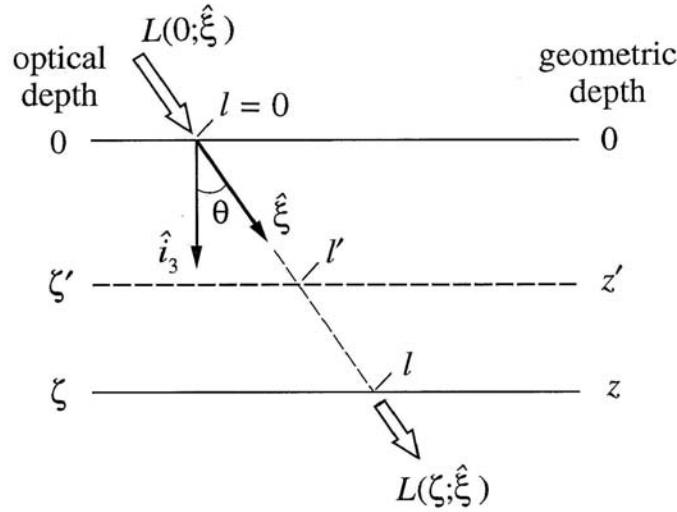
Fig. 5.2. Geometry relating optical depth ζ, optical path length l, and geometric depth z, as used to discuss the apparent radiance form of the RTE.

Equation (5.28) is also our first encounter with a *global formulation* of radiative transfer. In such a formulation, the radiance at depth ζ is expressed in terms of the known radiance on the boundary of the medium, here $L(0;\hat{\xi})$, and in terms of functions that specify the optical properties of *finitely thick* layers of water. In the present case, those functions are $T_l(\zeta;\hat{\xi})$ and $T_{l-l'}(\zeta - \zeta';\hat{\xi})$, which specify the transmission properties of water layers of thicknesses ζ and $\zeta-\zeta'$, respectively. Equation (5.24) is called a *local formulation* of the RTE because it relates the rate of change of the radiance, $dL/d\zeta$, at a given depth ζ to the optical properties of the water *at that* (local) *depth.* We shall encounter these ideas again in Chapters 7, 8 and 9.

We close this section with the remark that, had we chosen to derive the RTE using the linear interaction principle, we would have arrived at Eq. (5.29). The interaction principle would have guaranteed the existence of the *T* functions, just as it gave us the four surface reflectance and transmittance functions in Eqs. (4.3) and (4.4). We would have found that the *T* functions have the exponential forms seen in Eq. (5.28), from which we would have derived Eq. (5.24) by differentiation. This is the approach to the RTE taken in Chapter 3 of *H.O. II.* The development there, which starts from scratch and pays due attention to mathematical rigor, requires almost 200 pages to reach Eq. (5.29). This observation seems to recommend the heuristic approach followed in this chapter.

5.9 A Simple Model for Radiance

We already have encountered a very simple model for radiance distributions: Beer's law, which is exact only for purely absorbing media. We can obtain a more realistic (but still approximate) model for $L(z;\hat{\xi})$ if we incorporate scattering effects in some manner.

Consider a source-free, homogeneous water body, so that $S = 0$ and all IOP's are independent of depth; in particular, $c(z) = c$ and $\beta(z;\hat{\xi}'{\to}\hat{\xi}) = \beta(\hat{\xi}'{\to}\hat{\xi})$. Then the integral form (5.30) of the RTE reduces to

$$L(z;\hat{\xi}) = L(0;\hat{\xi}) \exp\left(-\frac{cz}{\mu}\right) + \int_0^z \frac{1}{\mu} L_*^{\mathrm{E}}(z';\hat{\xi}) \exp\left(-\frac{c(z - z')}{\mu}\right) dz' \quad (5.31)$$

In the absence of scattering, $L_*^{\mathrm{E}} = 0$ and the radiance decreases exactly exponentially with depth (Beer's law). Thus we may reason that the path function

$$L_*^{\mathrm{E}}(z;\hat{\xi}) = \int_\Xi L(z;\hat{\xi}') \beta(\hat{\xi}'{\to}\hat{\xi}) \, d\Omega(\hat{\xi}')$$

should also decrease *approximately* exponentially with depth, since β is independent of depth. So let us *assume* that

$$L_*^{\mathrm{E}}(z;\hat{\xi}) = L_*^{\mathrm{E}}(0;\hat{\xi}) e^{-Kz}, \quad (5.32)$$

where $K = K(\hat{\xi})$ is a positive constant (for a fixed direction $\hat{\xi}$) of dimension m^{-1}. Equation (5.32) has the same form as Eq. (3.21), which defined an average diffuse attenuation coefficient $\overline{K}_{\mathrm{d}}$ for downwelling plane irradiance. Since L_*^{E} determines the diffuse (or scattered) light field, we may anticipate that the K of Eq. (5.32) is closely related to the K-functions defined in Section 3.2.

Substitution of Eq. (5.32) into (5.31) allows the z' integration to be carried out. The result is

$$L(z;\hat{\xi}) = L(0;\hat{\xi}) \exp(-cz/\mu)$$
$$+ \frac{L_*^{\mathrm{E}}(0;\hat{\xi}) \exp(-cz/\mu)}{c - K\mu} \left\{ \exp\left[(c - K\mu)z/\mu\right] - 1 \right\},$$

or

$$L(z;\hat{\xi}) = L(0;\hat{\xi}) \exp(-cr)$$

$$+ \frac{L_*^E(0;\hat{\xi}) \exp(-Kr\cos\theta)}{c - K\cos\theta} \left\{ 1 - \exp[-(c - K\cos\theta)r] \right\}, \qquad (5.33)$$

where

$$r \equiv \frac{z}{\mu} = \frac{z}{\cos\theta} = \frac{l}{c} \qquad \text{(m)}$$

is the geometric distance along direction $\hat{\xi}$ from depth 0 to depth z. Equation (5.33) is the desired model for $L(z;\hat{\xi})$. This result is sometimes called the *classical canonical equation for radiance.*

Model (5.33) was first obtained by Preisendorfer (1964; see also *H.O. III*, Chapter 4), who presents theoretical arguments to support assumption (5.32), upon which the validity of Eq. (5.33) rests. The real test of the model of course lies in its ability to reproduce underwater radiance distributions. Figure 5.3 shows how well Eq. (5.33) fits one set of measurements of $L(z;\theta,\phi)$ taken on a clear sunny day with a level water surface (Tyler, 1960a). The values of $L_*^E(0;\theta,\phi)$ and of K, which are needed for evaluation of Eq. (5.33), were determined from additional measurements seen in Tyler (1960b). The agreement between the model and the data is remarkably good. Note in particular the behavior of the nadir radiance (photons leading downward in the $\theta = 0$ direction). Just below the water surface ($z \approx 0$), $L(z;0,\phi)$ consists mostly of transmitted sky light and of upwelling radiance reflected back downward by the surface; both of these quantities are relatively small. Therefore $L(z \approx 0;0,\phi)$ is small enough that the scattering term L_*^E (which is receiving a contribution from the large solar beam) is greater than the attenuation term $-cL$ in the RTE (5.22). Thus $dL/dz > 0$, and the radiance *increases* with depth. Below a certain depth, however, the exponential damping seen in Eq. (5.33) becomes dominant, and $L(z;0,\phi)$ begins to decrease with depth. This behavior can be reproduced by Eq. (5.33) because it contains a sum of exponentials. Beer's law, with only one exponential, always predicts L to decrease with depth. We shall comment again in Section 11.2 on this behavior of the nadir radiance.

The ability of Eq. (5.33) to mimic actual radiance distributions is all the more remarkable when we remember that Eq. (5.32) parametrizes the scattering process without making any assumptions about the nature of the volume scattering function β. But we must remember that Eq. (5.33) is a *diagnostic* equation; it cannot in general be used for *prediction*, because we do not know *a priori* the needed values of $L_*^E(0;\hat{\xi})$ and K. Equation (5.33)
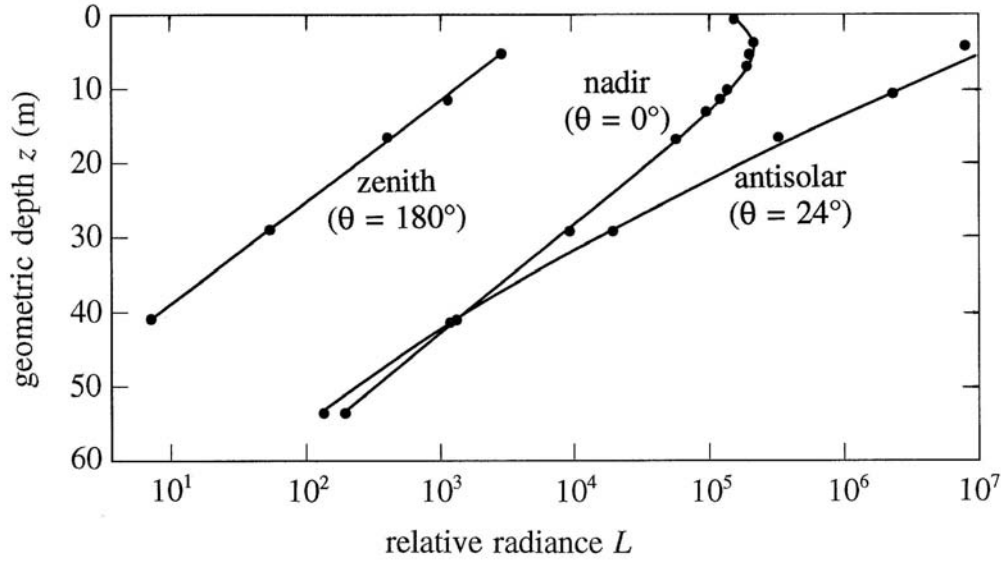
Fig. 5.3. Comparison of the radiance model of Eq. (5.33) (solid lines) with measured radiance values (dots), for three different θ values in the plane of the sun. Zenith, nadir, and antisolar refer to the directions of photon travel. [redrawn from Tyler (1960a)]

possesses predictive power only if $L_*^{\rm E}(0;\hat{\xi})$ and K can be estimated from models or obtained by measurement. The real value of Eq. (5.33) lies in the insight it gives us into the behavior of radiance distributions.

The asymptotic radiance distribution

One more bit of insight can be obtained from Eq. (5.33) by considering its form for very great depths, $z \rightarrow \infty$. Since in all deep natural waters, the radiance decreases with depth below some level where surface effects may dominate (as for the zenith radiance in Fig. 5.3), it follows that $c > K\cos\theta$ in Eq. (5.33). Thus the $\exp(-cr)$ terms will damp out faster than the $\exp(-Kr\cos\theta)$ terms, leaving just

$$L(z;\hat{\xi}) \underset{z\to\infty}{\rightarrow} \frac{L_*^{\rm E}(0;\hat{\xi})\, e^{-Kz}}{c - K\cos\theta} = \frac{L_*^{\rm E}(z;\hat{\xi})/c}{1 - \dfrac{K}{c}\cos\theta}\,.$$

This limiting form shows that $L(z;\theta,\phi)$ approaches the shape of a ellipse in θ, with eccentricity K/c, as modified by a factor depending on the IOP's of

the water body. This result is our first contact with the idea of an *asymptotic radiance distribution.* Preisendorfer (1959; see also *H.O. V*, Chapter 10) proves the general result that in all waters that are homogeneous below some finite depth, the radiance distribution at great depth approaches the form

$$L(z;\theta,\phi) \quad \underset{z \to \infty}{\to} \quad \frac{g(\theta)\exp(-k_\infty z)}{1 - \frac{k_\infty}{c}\cos\theta} \equiv L_\infty(\theta)\exp(-k_\infty z),$$

(5.34)

where k_∞ and $g(\theta)$ depend *only* on the inherent optical properties of the medium (and not on the boundary conditions). Thus the *shape* $L_\infty(\theta)$ of the radiance distribution approaches that of a solid of revolution with a vertical axis, and the *magnitude* of the radiance decreases exactly exponentially. We shall learn in Section 9.6 how to compute k_∞ and $L_\infty(\theta)$ from a given set of IOP's.

5.10 The Divergence Law for Irradiance

The radiance transfer equation is a statement of energy conservation in the sense that it accounts for all the losses and gains to a swarm of photons moving through the water in a fixed direction. We now derive a useful conservation statement that holds at a fixed point in the water, through which photons are moving in all directions.

The desired result is obtained by integrating the RTE (5.20) over all directions $\hat{\xi} \in \Xi$ and recalling the definitions of the various irradiances introduced in Section 1.5. The left hand side of Eq. (5.20) yields

$$\int_\Xi \mu \frac{dL}{dz}\, d\Omega(\hat{\xi}) = \frac{d}{dz}\int_\Xi L(z;\theta,\phi)\cos\theta\, d\Omega(\theta,\phi)$$

$$= \frac{d}{dz}(E_d - E_u),$$

after recalling Eqs. (1.23) and (1.24). The $-cL$ term in Eq. (5.20) becomes

$$\int_\Xi (-cL)\, d\Omega(\hat{\xi}) = -c(z)\int_\Xi L(z;\hat{\xi})\, d\Omega(\hat{\xi}) = -c(z)E_o(z),$$

where $E_o(z)$ is the scalar irradiance defined in Eq. (1.26). The elastic scatter path function gives

$$\int_\Xi L_*^{E} \, d\Omega(\hat{\xi}) \;=\; \int_\Xi \left[\int_\Xi L(z;\hat{\xi}') \, \beta(z;\hat{\xi}' \!\to\! \hat{\xi}) \, d\Omega(\hat{\xi}') \right] d\Omega(\hat{\xi})$$

$$=\; \int_\Xi L(z;\hat{\xi}') \left[\int_\Xi \beta(z;\hat{\xi}' \!\to\! \hat{\xi}) \, d\Omega(\hat{\xi}) \right] d\Omega(\hat{\xi}')$$

$$=\; b(z) \int_\Xi L(z;\hat{\xi}') \, d\Omega(\hat{\xi}')$$

$$=\; b(z) \, E_{o}(z) \,.$$

Here we have used Eqs. (5.4), (5.8), and (1.26). The inelastic scatter path function is reduced in a similar manner:

$$\int_\Xi L_*^{I} \, d\Omega(\hat{\xi}) \;=\; \int_\Xi \left[\int_\Xi \int_\Lambda L(z;\hat{\xi}';\lambda') \, \beta^{I}(z;\hat{\xi}' \!\to\! \hat{\xi};\lambda' \!\to\! \lambda) \, d\lambda' \, d\Omega(\hat{\xi}') \right] d\Omega(\hat{\xi})$$

$$=\; \int_\Xi \int_\Lambda L(z;\hat{\xi}';\lambda') \left[\int_\Xi \beta^{I}(z;\hat{\xi}' \!\to\! \hat{\xi};\lambda' \!\to\! \lambda) \, d\Omega(\hat{\xi}) \right] d\lambda' \, d\Omega(\hat{\xi}')$$

$$=\; \int_\Lambda b^{I}(z;\lambda' \!\to\! \lambda) \, E_{o}(z;\lambda') \, d\lambda' \,,$$

where we have used Eqs. (5.10) and (5.11). Finally, we define

$$\int_\Xi L_*^{S} \, d\Omega(\hat{\xi}) \;\equiv\; E_*^{S} \,.$$

Collecting terms resulting from the directional integration of the RTE, we have

$$\frac{d}{dz}(E_d - E_u) \;=\; -c E_o \;+\; b E_o \;+\; \int_\Lambda b^{I} E_o \, d\lambda' \;+\; E_*^{S} \,,$$

or

$$\frac{d}{dz}(E_d - E_u) \;=\; -a E_o \;+\; E_o^{S} \qquad (\text{W m}^{-3} \text{ nm}^{-1}) \,, \qquad (5.35)$$

which is the desired result. For convenience, we have grouped the inelastic scatter and the true emission term together into an effective source term

$$E_o^{S} \;\equiv\; \int_\Xi S(\hat{\xi}) \, d\Omega(\hat{\xi}) \,,$$

as was done in Eqs. (5.21) and (5.22). Starting with the general RTE (5.19) and assuming a constant index of refraction leads to

$$\frac{1}{v} \frac{\partial E_o}{\partial t} + \nabla \cdot \vec{E} = -a\, E_o + E_o{}^S , \qquad\qquad (5.36)$$

where $\vec{E}$ is the vector irradiance defined by Eq. (1.27). This equation, or its time-independent, one-dimensional form (5.35), is called the *divergence law* for irradiance. If there is no inelastic scatter and no internal sources, Eq. (5.35) reduces to

$$\frac{d}{dz} (E_d - E_u) = -a\, E_o , \qquad\qquad (5.37)$$

which is known as Gershun's law (1936, 1939).

The physical significance of Eq. (5.35) is that it relates the depth rate of change of the net irradiance $E_d - E_u$ to the absorption coefficient a, the scalar irradiance E_o, and any internal sources of radiant energy at the wavelength of interest. If the source term is zero or known, then Eq. (5.35) can be used to obtain the absorption coefficient a from *in situ* measurements of the irradiances E_d, E_u, and E_o. This is our first example of an *inverse model* – a model that retrieves an inherent optical property from measurements of the light field. Inverse models are the subject of Chapter 10.

Voss (1989) used Gershun's law (5.37) to recover a values to within an estimated error of order 20%. Inelastic scattering and internal source effects were reasonably assumed to be negligible in his study. The needed irradiances were all computed from a measured radiance distribution, so that no intercalibration of instruments was required. Maffione, *et al.* (1993) determined absorption values by writing the source-free form (i.e. $E_o{}^S = 0$) of the divergence law (5.36) in spherical coordinates and applying the result to irradiance measurements made using an underwater, artificial, *isotropic* light source. The artificial light source allowed measurements to be made at night, thus there was no inelastic scattering from other wavelengths. Their instrument did not require absolute radiometric calibration. However, Gershun's law will give *incorrect* absorption values if naively applied to waters and wavelengths where inelastic processes such as Raman scattering or fluorescence are significant. For this reason, and because of calibration difficulties if different instruments are used to measure E_d, E_u, and E_o, Gershun's law is seldom used as a way to measure absorption. It is, however, a useful check on the internal consistency of numerical models.

5.11 Irradiance Transfer: The Two-flow Equations

We now have seen several versions of the equation governing radiance transfer in natural waters. Even in its simplest useful form, Eq. (5.22), the RTE is rather intimidating when written out in its full glory, as in Eq. (5.23). But, if we want to accurately predict the radiance distribution, we have to solve the RTE regardless of the effort required. However, for many purposes in hydrologic optics, knowledge of irradiances (e.g. E_d and E_u, or E_o) is sufficient. Thus we ask if it is possible to develop predictive equations governing irradiances. Presumably such irradiance transfer equations would be simpler that the RTE, since irradiance does not contain the detailed directional information inherent in the radiance distribution. We could then solve these irradiance transfer equations and directly obtain the desired irradiances, without having to first compute the full radiance distribution. We shall see in this section to what extent this goal can be achieved.

Heuristic derivation

Let us see if we can develop a pair of irradiance transfer equations governing the depth behavior of the downwelling and upwelling spectral plane irradiances, $E_d(z;\lambda)$ and $E_u(z;\lambda)$, which were defined in Section 1.5. We will obtain valuable guidance for their subsequent rigorous mathematical development if we can first deduce the general form that such a pair of equations must have. For simplicity, let us consider the case of no transpectral scatter and no internal sources. We omit the wavelength argument for brevity.

We need two equations for the two irradiances. At any given depth z, the depth-rate-of-change of E_d should comprise two parts. The first part would describe a decrease in E_d owing to absorption or to elastic scattering of photons from downward into upward directions. The second term would describe an increase in E_d owing to the elastic scattering of photons from upward into downward directions. Thus the equation should have the form

$$\frac{dE_d(z)}{dz} \;=\; \tau_{dd}(z)\,E_d(z) \;+\; \rho_{ud}(z)\,E_u(z)\,. \qquad (5.38)$$

Here τ_{dd} describes the photons originally heading downward (the first subscript) that continue to head downward (the second subscript), or that are absorbed at level z. We anticipate that τ_{dd} will be negative, since it is the only "loss" term in the equation, and since E_d in general decreases with

depth (i.e. $dE_d/dz < 0$). The quantity ρ_{ud} describes how photons originally heading upward (those that form E_u) get scattered into downward directions. This quantity represents a "gain," and thus should be positive. The same line of reasoning suggests an equation of the form

$$ -\frac{dE_u(z)}{dz} = \tau_{uu}(z)\,E_u(z) + \rho_{du}(z)\,E_d(z) \qquad (5.39) $$

for the depth derivative of E_u. The minus sign on the left-hand side of the equation is inserted in anticipation of its rigorous derivation below, where its origin will be seen. Once again, we expect $\tau_{uu} < 0$ and $\rho_{du} > 0$. Equations (5.38) and (5.39) are called the *two-flow equations for irradiance* because all the directions of photon "flow" are grouped into two categories: upward or downward flow.

The two-flow equations are often called *two-stream* equations. However, the word "stream" brings to mind a narrow beam of photons traveling in a given direction, rather than photons traveling in all directions within a hemisphere. With this connotation, a two-stream model would compute the radiance in two specific directions, say the nadir and zenith directions. Such models can be formulated; see, for example, Liou (1980), who develops in detail the equations governing the azimuthally averaged *radiances* in the two stream directions $\mu = \pm 0.577$ ($\theta = \pm 54.7°$). These stream directions arise naturally in the solution of the RTE by the discrete ordinates method, to be discussed in Section 9.1. This distinction between "two-flow" and "two-stream" models is not usually made in the literature.

Note that the four coefficients τ_{dd}, τ_{uu}, ρ_{du}, and ρ_{ud} are all distinct. These quantities depend (in some fashion as yet unknown) on the water's inherent absorption and scattering properties, which are independent of direction. But they also depend on the directional distribution of the photons generating E_d and E_u. The directional distribution of upwelling photons is in general different than the distribution of photons heading downward, as illustrated in Fig. 5.4. Thus, for example, there is no reason to expect that the quantity ρ_{du}, which describes how downwelling irradiance gets converted into upwelling irradiance, will be equal to the quantity ρ_{ud}, which describes how upwelling irradiance gets converted into downwelling irradiance.

The quantities τ_{dd} and ρ_{du} are respectively called the *local transmittance* and *local reflectance functions for downwelling irradiance*; τ_{uu} and ρ_{ud} are the corresponding functions for *upwelling irradiance*. We shall encounter these functions (and their radiance counterparts) many times in our subsequent work.
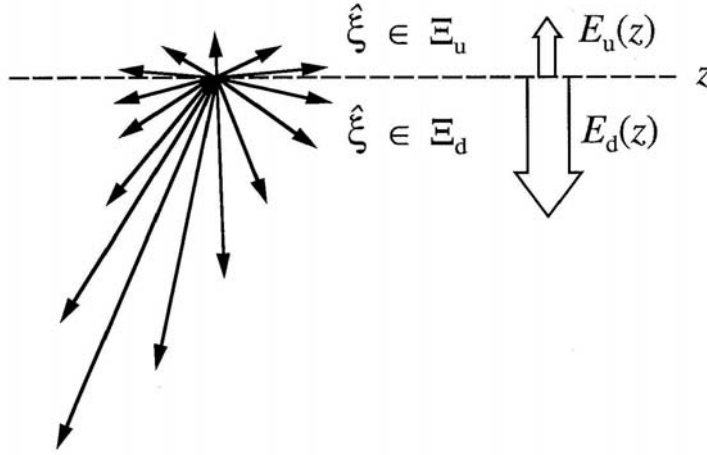
Fig. 5.4.   Illustration of the directional distributions of photons in the downwelling and upwelling hemispheres.

Rigorous derivation

If our intuitive arguments in the previous paragraphs are correct, we should be able to derive equations of the form of Eqs. (5.38) and (5.39) by rigorous manipulation of the RTE (5.23). We begin by integrating Eq. (5.23) over all directions $\hat{\xi}$ in the downward hemisphere Ξ_d. Clearly,

$$\int_{\Xi_d} \mu\, \frac{dL(z;\hat{\xi})}{dz}\, d\Omega(\hat{\xi}) \;=\; \frac{dE_d(z)}{dz}\,,$$

and

$$\int_{\Xi_d} \left[-c(z)\,L(z;\hat{\xi})\right] d\Omega(\hat{\xi}) \;=\; -c(z)\,E_{od}(z)\,.$$

For convenience of notation, let the Ξ_d integral of the effective radiance source term be

$$E_{od}^{S}(z) \;\equiv\; \int_{\Xi_d} S(z;\hat{\xi})\, d\Omega(\hat{\xi})\,,$$

which we call the *effective source term for downwelling irradiance.* The path function term L_*^{E} becomes (dropping the depth argument)

$$\int\limits_{\Xi_d} \left[\int\limits_{\Xi} L(\hat{\xi}') \, \beta(\hat{\xi}' {\to} \hat{\xi}) \, d\Omega(\hat{\xi}') \right] d\Omega(\hat{\xi})$$

$$= \int\limits_{\Xi_d} \left[\int\limits_{\Xi_d} L \, \beta \, d\Omega(\hat{\xi}') + \int\limits_{\Xi_u} L \, \beta \, d\Omega(\hat{\xi}') \right] d\Omega(\hat{\xi}) \, .$$

This is as far as we can go by blind manipulation of the RTE.

To proceed, let us recall the desired form of Eq. (5.38) and note that the term

$$\int\limits_{\Xi_d} \int\limits_{\Xi_d} L(\hat{\xi}') \, \beta(\hat{\xi}' {\to} \hat{\xi}) \, d\Omega(\hat{\xi}') \, d\Omega(\hat{\xi})$$

in the last equation describes how much of the downwelling radiance is scattered into downward directions. This term must therefore be related to the $\tau_{dd} E_d$ term in Eq. (5.38). Likewise, the term

$$\int\limits_{\Xi_d} \int\limits_{\Xi_u} L(\hat{\xi}') \, \beta(\hat{\xi}' {\to} \hat{\xi}) \, d\Omega(\hat{\xi}') \, d\Omega(\hat{\xi})$$

must be related to the $\rho_{ud} E_u$ term in Eq. (5.38).

Let us now define the (elastic) *diffuse forward scattering function for downwelling irradiance* as

$$f_{dd} \equiv \frac{1}{E_d} \int\limits_{\Xi_d} \int\limits_{\Xi_d} L(\hat{\xi}') \, \beta(\hat{\xi}' {\to} \hat{\xi}) \, d\Omega(\hat{\xi}') \, d\Omega(\hat{\xi}) \qquad (\text{m}^{-1}) \, , \qquad (5.40)$$

and define the (elastic) *diffuse backward scattering function for upwelling irradiance* as

$$b_{ud} \equiv \frac{1}{E_u} \int\limits_{\Xi_d} \int\limits_{\Xi_u} L(\hat{\xi}') \, \beta(\hat{\xi}' {\to} \hat{\xi}) \, d\Omega(\hat{\xi}') \, d\Omega(\hat{\xi}) \qquad (\text{m}^{-1}) \, . \qquad (5.41)$$

Finally, let us define the *diffuse attenuation function for downwelling irradiance* as

$$c_d \equiv c \, \frac{E_{od}}{E_d} = c \, D_d = \frac{c}{\bar{\mu}_d} \qquad (\text{m}^{-1}) \, . \qquad (5.42)$$

Here $D_d = 1/\bar{\mu}_d$ is the distribution function for downwelling irradiance defined in Eq. (3.16); $\bar{\mu}_d$ is the downwelling average cosine defined in Eq. (3.14).

If we now collect terms and use definitions (5.40)-(5.42), the Ξ_d-integrated RTE becomes

$$\frac{dE_d}{dz} = \left(f_{dd} - c_d\right)E_d + b_{ud}E_u + E_{od}^S.$$

(5.43)

In the source-free case, this equation has the form of Eq. (5.38), and so we can make the identifications

$$\tau_{dd} = f_{dd} - c_d$$
$$\rho_{ud} = b_{ud}.$$

(5.44)

Equations (5.44) and (5.40)-(5.42) show exactly how the local transmittance τ_{dd} and reflectance ρ_{ud} postulated in Eq. (5.38) depend on the inherent optical properties c and β, and on the directional structure of the radiance distribution.

We now return to the RTE (5.23) and integrate over all directions in the upward hemisphere Ξ_u. The derivative term is

$$\int_{\Xi_u} \mu \, \frac{dL(z;\hat{\xi})}{dz} \, d\Omega(\hat{\xi}) = -\frac{dE_u}{dz}.$$

Here we have noted that $\mu < 0$ when $\hat{\xi} \in \Xi_u$; this is the origin of the minus sign placed in Eq. (5.39). This sign is a vestige of the general convention to measure optical path length l as positive in the direction of $\hat{\xi}$. For upward directions, $\hat{\xi} \in \Xi_u$, depth z decreases as l increases, and the sign accounts for a negative dz corresponding to a positive dl.

The remainder of our derivation proceeds in parallel with the one leading to Eq. (5.42). The result is

$$-\frac{dE_u}{dz} = \left(f_{uu} - c_u\right)E_u + b_{du}E_d + E_{ou}^S,$$

(5.45)

where

$$f_{uu} \equiv \frac{1}{E_u} \int_{\Xi_u} \int_{\Xi_u} L(\hat{\xi}') \, \beta(\hat{\xi}'{\to}\hat{\xi}) \, d\Omega(\hat{\xi}') \, d\Omega(\hat{\xi})$$

(5.46)

is the *diffuse forward scattering function for upwelling irradiance*,

$$b_{du} \equiv \frac{1}{E_d} \int_{\Xi_u} \int_{\Xi_d} L(\hat{\xi}') \, \beta(\hat{\xi}'{\to}\hat{\xi}) \, d\Omega(\hat{\xi}') \, d\Omega(\hat{\xi})$$

(5.47)

is the *diffuse backward scattering function for downwelling irradiance*,

$$c_{\mathrm{u}} \equiv c \frac{E_{\mathrm{ou}}}{E_{\mathrm{u}}} = c D_{\mathrm{u}} = \frac{c}{\bar{\mu}_{\mathrm{u}}} \tag{5.48}$$

is the *diffuse attenuation function for upwelling irradiance*, and

$$E_{\mathrm{ou}}^{\mathrm{S}} \equiv \int\limits_{\Xi_u} S(\hat{\xi}) \, d\Omega(\hat{\xi})$$

is the *effective source term for upwelling irradiance.* D_{u} and $\bar{\mu}_{\mathrm{u}}$ are respectively the upwelling distribution function and mean cosine, as defined in Eqs. (3.16) and (3.15). As before, we can identify

$$\tau_{\mathrm{uu}} = f_{\mathrm{uu}} - c_{\mathrm{u}}$$

$$\rho_{\mathrm{du}} = b_{\mathrm{du}} . \tag{5.49}$$

Have we now achieved our goal of obtaining a pair of equations that can be solved to obtain E_{d} and E_{u} given the IOP's of a water body, the source functions, and suitable boundary conditions on E_{d} and E_{u}? The answer is *no*. The four τ's and ρ's of Eqs. (5.38) and (5.39), or their equivalent *f*'s, *b*'s and *c*'s of Eqs. (5.43) and (5.45), are *apparent* optical properties. As the definitions of these quantities clearly show, they depend not just on the IOP's but also on the radiance distribution itself. Thus *the τ's and ρ's, which are needed before we can solve the two-flow irradiance equations, cannot be evaluated until the radiance distribution is known* – i.e. until we solve the RTE. Of course, if we solve the RTE and obtain the radiance, we can compute the desired irradiances immediately, and there is no need for the two-flow equations. Alas.

The alert reader will detect something suspicious about the above results. If the IOP's provide us with sufficient information to solve the RTE and find the radiance distribution, from which we can get the irradiances, why then are the IOP's *not* sufficient for a solution of the two-flow equations? It seems that we have somehow "lost" information.

The resolution of our quandary lies in the term

$$\int\limits_{\Xi_d} \left[-c L(\hat{\xi}) \right] d\Omega(\hat{\xi}) = -c E_{\mathrm{od}} ,$$

which we rewrote as

$$-c E_{\mathrm{od}} = -c_{\mathrm{d}} E_{\mathrm{d}} ,$$

after defining c_d in Eq. (5.42). In our straightforward integration of the RTE over Ξ_d, we obtained a term in E_{od}, where we needed a term proportional to E_d. We obtained the needed form by an *ad hoc* introduction of the mean cosine $\bar{\mu}_d$ in Eq. (5.42). This well-intended bit of analytic legerdemain is the source of our misery, since we do not know $\bar{\mu}_d$. Viewed from the information standpoint, we did indeed destroy information about the directional structure of the light field when we integrated over all directions $\hat{\xi}$ in Ξ_d. Similar comments hold for Eq. (5.48) and $\bar{\mu}_u$.

We have replaced a complicated equation (the RTE) requiring simple input (the IOP's) with simple equations (the two-flow equations) requiring complicated input (the τ's and ρ's). We can solve the two-flow equations only if we can some way determine the needed τ's and ρ's, and this requires information *in addition* to the IOP's required to solve the RTE. In essence, we must replace the information lost in the directional integration of the RTE.

In light of the above comments, are the two-flow equations of any value? Yes [see Supplementary Note 9]. In particular, the two-flow equations:

- provide a simple conceptual framework for understanding irradiance behavior in natural waters. Their very derivation highlights the roles played by various radiative transfer processes, and we shall gain much additional insight from these equations in the following pages.

- can be manipulated to obtain several useful relations between inherent and apparent optical properties, as we shall see in Section 5.11.

- provide a simple mathematical setting for our development of invariant imbedding theory, a powerful mathematical technique for the solution of the radiance transfer equation. We shall pursue this matter beginning in Chapter 7.

- provide a simple mathematical framework for the development of inverse models for obtaining IOP's from measured AOP's. Such models are the subject matter of Chapter 10.

Alternate forms of the two-flow equations

We have encountered several simple relations between the IOP's. For example,

$$ c = a + b = a + b_f + b_b, \tag{5.50} $$

where b_f and b_b are the forward and backward scattering coefficients defined by Eq. (3.6). We now show that similar simple relations hold for the AOP's f_dd, b_du, c_d, etc. Consider $f_\text{dd} + b_\text{du}$:

$$f_\text{dd} + b_\text{du} = \frac{1}{E_\text{d}} \int_{\Xi_d} \int_{\Xi_d} L(\hat{\xi}') \, \beta(\hat{\xi}' \!\to\! \hat{\xi}) \, d\Omega(\hat{\xi}') \, d\Omega(\hat{\xi})$$

$$+ \frac{1}{E_\text{d}} \int_{\Xi_u} \int_{\Xi_d} L(\hat{\xi}') \, \beta(\hat{\xi}' \!\to\! \hat{\xi}) \, d\Omega(\hat{\xi}') \, d\Omega(\hat{\xi})$$

$$= \frac{1}{E_\text{d}} \int_{\Xi_d} L(\hat{\xi}') \left[\int_{\Xi_d} \beta(\hat{\xi}' \!\to\! \hat{\xi}) \, d\Omega(\hat{\xi}) + \int_{\Xi_u} \beta(\hat{\xi}' \!\to\! \hat{\xi}) \, d\Omega(\hat{\xi}) \right] d\Omega(\hat{\xi}')$$

$$= \frac{b}{E_\text{d}} \int_{\Xi_d} L(\hat{\xi}') \, d\Omega(\hat{\xi}') = b \frac{E_\text{od}}{E_\text{d}}.$$

Here we used Eq. (5.8) to reduce the $\hat{\xi}$ integral in brackets. This last equation suggests that we define a *total diffuse scattering function for downwelling irradiance* as

$$b_\text{d} \equiv b \frac{E_\text{od}}{E_\text{d}} = b \, D_\text{d} = \frac{b}{\bar{\mu}_\text{d}}.$$

Likewise, we can define a *diffuse absorption function for downwelling irradiance* as

$$a_\text{d} \equiv a \frac{E_\text{od}}{E_\text{d}} = a \, D_\text{d} = \frac{a}{\bar{\mu}_\text{d}}. \tag{5.51}$$

With these definitions we can write

$$c_\text{d} = a_\text{d} + b_\text{d}$$
$$= a_\text{d} + f_\text{dd} + b_\text{du}. \tag{5.52}$$

Corresponding definitions for the upwelling irradiance yield

$$a_\text{u} \equiv a \frac{E_\text{ou}}{E_\text{u}} = a \, D_\text{u} = \frac{a}{\bar{\mu}_\text{u}},$$

$$b_\text{u} \equiv b \frac{E_\text{ou}}{E_\text{u}} = b \, D_\text{u} = \frac{b}{\bar{\mu}_\text{u}},$$

and

$$c_\text{u} = a_\text{u} + b_\text{u}$$
$$= a_\text{u} + f_\text{uu} + b_\text{ud}. \tag{5.53}$$

Equations (5.52) and (5.53) both correspond to Eq. (5.50). These equations allow us to write Eqs. (5.43) and (5.45) as

$$\frac{dE_d}{dz} = -\left(a_d + b_{du}\right)E_d + b_{ud}E_u + E_{od}^{S} \tag{5.54}$$

$$-\frac{dE_u}{dz} = -\left(a_u + b_{ud}\right)E_u + b_{du}E_d + E_{ou}^{S}. \tag{5.55}$$

This form of the two-flow equations displays their underlying physics. In Eq. (5.54), we see that E_d

(i)   decreases with depth because of absorption of E_d,

(ii)   decreases with depth because of scattering of E_d into E_u (note that this loss from E_d appears as a gain in the equation for E_u),

(iii) increases with depth because of scattering of E_u into E_d (note that this gain here is a loss in the equation for E_u),

(iv)   increases with depth because of internal sources of E_d.

A similar interpretation holds for Eq. (5.55).

The effective internal source terms E_{od}^{S} and E_{ou}^{S} can be expanded to show explicitly the contributions by inelastic scatter and by true emission. Consider, for example,

$$E_{od}^{S}(\lambda) \equiv \int_{\Xi_d} S(\hat{\xi};\lambda)\, d\Omega(\hat{\xi})$$

$$= \int_{\Xi_d} \left[L_*^{I} + L_*^{S}\right] d\Omega(\hat{\xi}). \tag{5.56}$$

Recalling Eq. (5.10) for L_*^{I} and defining the *inelastic diffuse forward and backward scattering functions*

$$f_{dd}^{I}(\lambda' {\to} \lambda) \equiv \frac{1}{E_d(\lambda')} \int_{\Xi_d}\int_{\Xi_d} L(\hat{\xi}';\lambda')\, \beta^{I}(\hat{\xi}'{\to}\hat{\xi};\lambda'{\to}\lambda)\, d\Omega(\hat{\xi}')\, d\Omega(\hat{\xi}) \tag{5.57}$$

$$b_{ud}^{I}(\lambda' {\to} \lambda) \equiv \frac{1}{E_u(\lambda')} \int_{\Xi_d}\int_{\Xi_u} L(\hat{\xi}';\lambda')\, \beta^{I}(\hat{\xi}'{\to}\hat{\xi};\lambda'{\to}\lambda)\, d\Omega(\hat{\xi}')\, d\Omega(\hat{\xi}) \tag{5.58}$$

$$(\mathrm{m}^{-1}\, \mathrm{nm}^{-1}),$$

reduces Eq. (5.56) to

$$E_{od}^{S}(\lambda) = \int_{\Lambda} f_{dd}^{I}(\lambda' \rightarrow \lambda) \, E_{d}(\lambda') \, d\lambda$$

$$+ \int_{\Lambda} b_{ud}^{I}(\lambda' \rightarrow \lambda) \, E_{u}(\lambda') \, d\lambda' \; + \int_{\Xi_{d}} L_{*}^{S}(\hat{\xi};\lambda) \, d\Omega(\hat{\xi}) \, . \qquad (5.59)$$

This equation shows three internal sources of downwelling irradiance:

(i)   downwelling irradiance $E_{d}(\lambda')$ that is inelasticly forward scattered into $E_{d}(\lambda)$,

(ii)   upwelling irradiance $E_{u}(\lambda')$ that is inelasticly backscattered into $E_{d}(\lambda)$,

(iii) true emission of photons into downward directions.

Corresponding equations for E_{ou}^{S} can be obtained by interchanging "u" and "d" in Eqs. (5.56)-(5.59).

  We now have seen three forms of the two-flow equations: Eqs. (5.38) and (5.39), (5.43) and (5.45), and (5.54) and (5.55). Each form sheds a slightly different light on the inner workings of the equations. It is important to recognize that the equations derived above are the *most general forms* of the two-flow equations governing E_{d} and E_{u}. These equations are *exact*, given the definitions of the *four independent parameters* a_{u}, a_{d}, b_{ud} and b_{du} (or their equivalent) and the *two source terms* E_{od}^{S} and E_{ou}^{S}. Simplifications of these equations often are made in particular applications, in order to make the equations solvable, but any simplifications must be carefully justified.

  In Chapter 7 we shall consider the boundary conditions associated with the two-flow equations.

Significance of the diffuse absorption and scattering functions

  In the preceding pages we encountered some rather confusing notation: b_{f} and b_{b} for the forward and backward scattering coefficients, which are IOP's; b_{du} and b_{ud} for the diffuse backscattering functions for downwelling and upwelling irradiances, which are AOP's, and so on. Even b_{b} alone is bad enough: the mainline "b" stands for "scattering" and the subscript "b" stands for "backward." In spite of its poor design in having the same letter denote two different concepts, we use b_{b} because it is the IAPSO recommended notation now in wide use. We use b_{du} and b_{ud}, for example, because the subscripts immediately identify the relevant

hemispheres of directions, Ξ_d and Ξ_u. Alternative notation, such as that used in *H.O.*, is equally confusing.

It is very important to understand the physical significance of the various absorption and scattering functions and coefficients. Consider, for example, a_d as defined by Eq. (5.51). The "beam" absorption coefficient *a* defined in Eq. (3.1) measures how strongly light is absorbed from a single, collimated beam per unit distance traveled by the beam; the direction of the beam is irrelevant. The diffuse absorption function a_d measures how strongly *downwelling irradiance* is absorbed per unit of *vertical* distance, i.e. per unit depth in the plane-parallel water body. A photon traveling downward from depth z_1 to depth z_2 along a path inclined at an angle θ from the nadir direction travels a distance $(z_2-z_1)/\cos\theta$. Its chance of being absorbed in thus increased by a factor of $1/\cos\theta$, compared to a photon heading straight downward in going from z_1 to z_2. The downward-traveling photons, which together generate E_d, on average have $\cos\theta = \bar{\mu}_d$. Thus on average they have their absorption increased by a factor of $1/\bar{\mu}_d$ in traveling from z_1 to z_2. This enhancement of absorption for E_d owing to the directions of photon travel gives the physical interpretation of a_d. Similar comments hold for upward-traveling photons and a_u. However, because the downward and upward traveling photons generally have different average cosines, E_d and E_u are absorbed at different rates per unit vertical distance; thus $a_d \neq a_u$. The quantities b_d, b_u, c_d and c_u reflect corresponding increases over the respective IOP's *b* and *c*.

The diffuse backscattering functions b_{du} and b_{ud} are more subtle. Consider, for example, b_{du}, which measures how strongly downward-traveling photons are converted into upward-traveling photons. The subtlety lies in the observation that b_{du} is determined in part by *forward-scattered* photons. This is illustrated in Fig. 5.5. In the figure, the heavy arrow represents $L(z;\theta',\phi')$ for a given direction $\hat{\xi}' = (\theta',\phi')$, and the oval line represents the radiance scattered into all direction $\hat{\xi} = (\theta,\phi)$ at depth *z*. The dashed line separates forward and backward scattering directions relative to the given $\hat{\xi}'$. The light arrows denote radiance scattered *upward* from the *downwelling* direction $\hat{\xi}'$. It is this radiance that represents the conversion of E_d into E_u, or in other words that determines b_{du} (when all downward directions $\hat{\xi}' \in \Xi_d$ are considered). Likewise, note that some backscattered radiance continues to head downward, and thus contributes to f_{dd}. The reason for using two subscripts on b_{du} is to emphasize that b_{du} *describes scattering from downward to upward directions, which is not the same as backscattering* (scattering through scattering angles of $\psi \geq 90°$). Similar comments hold for b_{ud}, f_{dd} and f_{uu}. The quantities b_{du} and b_{us} are
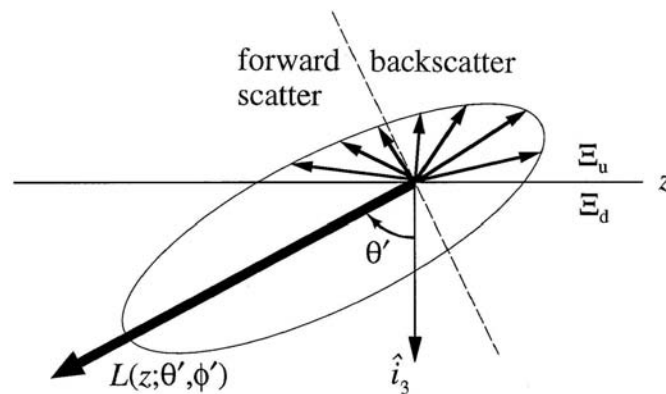
Fig. 5.5. Schematic diagram showing how both forward and backward scattering contribute to b_{du}, the diffuse backward scattering function for downwelling irradiance.

related to the shape factors introduced by Aas (1987) and by Stavn and Weidemann (1989). We shall discuss this connection in Section 10.3.

Because of the diverse applications of the two-flow equations, there is much variation in the terminology associated with them. Many authors call b_{du} (or some simplification thereof) "the backscatter." This is understandable since, for example, in an atmospheric application, b_{du} at a given depth tells how much of the downwelling irradiance at that depth is scattered back towards space – a quantity of great interest. Wiscombe and Grams (1976) have commented on the confusion associated with the term "backscatter" as used in atmospheric optics (their "backscattered fraction" is our b_{du} for an assumed hemispherically isotropic radiance distribution). We shall learn in Chapter 7 that it is also very important to distinguish between the *local* reflectance function $\rho_{du} = b_{du}$ of an *infinitesimal* layer of matter and the *global* reflectance function for a *finite-depth* layer of matter. Table 5.2 compares our notation for the various diffuse absorption and scattering functions with that used in several recent works in hydrologic optics.

Many users of two-flow equations have derived them *de novo* for their particular application, using arguments like those we presented in our heuristic derivation. Most such derivations fail (either inadvertently or through carefully stated assumptions) to account for the differences in the upward and downward radiance distributions, and thus arrive at a "two-parameter" set of equations. The two parameters are an absorption-like

Table 5.2. Notations used by various authors for the parameters appearing in the two-flow equations.

this book	H.O.[a] (1977)	Kirk (1981)	Aas (1987)	Stavn and Weidemann (1989)
a_d	$a(z,-)$	a_d	a_d	$a/\bar{\mu}_d$
a_u	$a(z,+)$	a_u	a_u	$a/\bar{\mu}_d$
b_d	$s(z,-)$	—	—	—
b_u	$s(z,+)$	—	—	—
b_{du}	$b(z,+)$	b_{bd}	b_d	$\bar{b}_d/\bar{\mu}_d$
b_{ud}	$b(z,-)$	b_{bu}	b_u	$\bar{b}_u/\bar{\mu}_u$
c_d	$\alpha(z,-)$	—	c_d	—
c_u	$\alpha(z,+)$	—	c_u	—

a. *H.O.* (Preisendorfer, 1977) uses "+" for upward, "−" for downward.

quantity, which replaces a_u and a_d, and a scattering-like quantity, which replaces b_{ud} and b_{du}.

We note in closing this section that Preisendorfer (1958b) first derived the general two-flow equations from an integration of the RTE. He repeated this derivation in his monograph (Preisendorfer, 1965) and again in detail in *H.O. V.* His derivation was well known in the hydrologic optics community. Yet as late as 1981, Acquista, *et al.* (1981, quoted by permission) were able to state in an atmospheric optics paper that "... it is not widely recognized that Schuster's approximation [a two-parameter version of the two-flow equations; see Section 5.17] can be derived from the exact transfer equation in a mathematically rigorous fashion." They then rigorously rederived Schuster's version of the two-flow equations and went on to discretize the RTE (as we shall do in Chapter 8) in a manner that corresponds to the quad-averaging scheme developed (or rediscovered) by Preisendorfer and Mobley in the mid-1980's. Sometimes knowledge diffuses slowly in both directions.

5.12 Relations Among IOP's and AOP's

In Section 3.2 we defined several apparent optical properties (AOP's) that find frequent application in hydrologic optics. Among these are the *K*-functions for downward and upward plane irradiance [Eq. (3.20)],

$$K_d = -\frac{1}{E_d}\frac{dE_d}{dz} \qquad (\text{m}^{-1}), \tag{5.60}$$

$$K_u = -\frac{1}{E_u}\frac{dE_u}{dz} \qquad (\text{m}^{-1}), \tag{5.61}$$

the irradiance reflectance [Eq. (3.17)],

$$R \equiv \frac{E_u}{E_d}, \tag{5.62}$$

and the mean cosines [Eqs. (3.14) and (3.15)] and distribution functions [Eq.(3.16)],

$$\bar{\mu}_d \equiv \frac{E_d}{E_{od}} = \frac{1}{D_d}, \tag{5.63}$$

$$\bar{\mu}_u \equiv \frac{E_u}{E_{ou}} = \frac{1}{D_u}. \tag{5.64}$$

The two-flow irradiance equations yield several useful relations among these AOP's and the IOP's, for the case of no internal sources. Simply dividing the source-free forms of Eqs. (5.54) and (5.55) by E_d and E_u, respectively, and using the above definitions gives

$$K_d = \frac{a}{\bar{\mu}_d} + b_{du} - b_{ud}R, \tag{5.65}$$

$$-K_u = \frac{a}{\bar{\mu}_u} + b_{ud} - \frac{b_{du}}{R}, \tag{5.66}$$

which connect the K's, $\bar{\mu}$'s, and R with the absorption and scattering properties of the medium. Adding Eqs. (5.54) and (5.55), dividing the resulting equation by E_d, and simplifying yields the very useful relation

$$R = \frac{K_d - a/\bar{\mu}_d}{K_u + a/\bar{\mu}_u} \tag{5.67}$$

connecting the K's, $\bar{\mu}$'s, and R to the absorption coefficient a of the water.

Gershun's law (5.37) can be rewritten in the equivalent forms

$$\bar{\mu} = \frac{a(1-R)}{K_d - RK_u} \tag{5.68}$$

and

$$\bar{\mu} = \frac{a}{K_{net}}, \qquad (5.69)$$

where K_{net} is the *K*-function for the net irradiance $E_d - E_u$.

The definition of $\bar{\mu}$,

$$\bar{\mu} \equiv \frac{E_d - E_u}{E_{od} + E_{ou}},$$

is easily manipulated to obtain

$$\bar{\mu} = \frac{1 - R}{\dfrac{1}{\bar{\mu}_d} + \dfrac{R}{\bar{\mu}_u}}.$$

The above relations are exact, to the accuracy with which internal sources can be ignored.

The source-free version of Eq. (5.43) can be manipulated as follows:

$$\frac{dE_d}{dz} = -c_d E_d + f_{dd} E_d + b_{ud} E_u$$

$$= -c_d E_d + \int_{\Xi_d}\int_{\Xi_d} L \beta \, d\Omega(\hat{\xi}') \, d\Omega(\hat{\xi}) + \int_{\Xi_d}\int_{\Xi_u} L \beta \, d\Omega(\hat{\xi}') \, d\Omega(\hat{\xi})$$

$$= -c_d E_d + \int_{\Xi_d}\left[\int_{\Xi} L \beta \, d\Omega(\hat{\xi}')\right] d\Omega(\hat{\xi})$$

$$= -c_d E_d + \int_{\Xi_d} L_*^{\mathrm{E}} \, d\Omega(\hat{\xi}),$$

or

$$K_d = c_d - \frac{1}{E_d}\int_{\Xi_d} L_*^{\mathrm{E}} \, d\Omega(\hat{\xi}).$$

Here we have used Eqs. (5.40), (5.41) and (5.8). The path function L_*^{E}, and hence the integral in the last equation, is never negative. Thus we can conclude that

$$K_d \le c_d,$$

or

$$K_d \bar{\mu}_d \le c, \qquad (5.70)$$

always. (Note that this conclusion is still valid in the presence of internal sources $E_{od}{}^{S}$.) The equality holds only in the idealized case of no scattering (and no internal sources). We already have seen a specific instance of this result in our discussion of the asymptotic radiance distribution in Section 5.8.

Rewriting Eq. (5.67) as

$$R(K_u + a/\bar{\mu}_u) + a/\bar{\mu}_d = K_d ,$$

we conclude that

$$a/\bar{\mu}_d \leq K_d$$

whenever $K_u \geq 0$. Combining this result with Eq. (5.70) yields

$$a \leq K_d \bar{\mu}_d \leq c \quad \text{(generally true)} . \tag{5.71}$$

The corresponding set of inequalities based on Eq. (5.45) is

$$a \leq -K_u \bar{\mu}_u \leq c \quad \text{(not generally true)} . \tag{5.72}$$

Once again, the right inequality always holds; the left is valid only when $K_d \leq 0$. Note that the left inequality, valid for $K_d \leq 0$, implies that $K_u \leq 0$ also, since the absorption coefficient a is always positive; i.e.

$$K_d \leq 0 \quad \Rightarrow \quad K_u \leq 0 .$$

The conditions under which $K_d \leq 0$ and $K_u \leq 0$ might occur warrant discussion. Negative K_d and K_u imply that E_d and E_u are *increasing* with depth z. Irradiances can certainly increase with depth if internal sources such as bioluminescence are present. However, we are for the moment considering only source-free waters. Upwelling irradiance also can increase with depth near highly reflecting bottoms (made of white sand, for example) in shallow waters. But can irradiances ever increase with depth in *deep* waters if no internal sources are present? In principle, they can. For example, we can envision that just below the surface in highly scattering water, the downwelling solar beam could be backscattered so strongly that E_u would increase with depth until the direct solar beam is sufficiently attenuated. Such behavior can be simulated in numerical models, but only under extreme conditions, such as single-scattering albedos of $\omega_o > 0.99$. It is unlikely that such conditions ever occur in natural waters. Thus we can reasonably assume that K_d and K_u are always positive. Therefore, in deep

natural waters, both inequalities of Eq. (5.71) hold. However, the left inequality of Eq. (5.72) is generally invalid, and the right inequality is trivial (a negative number is always less than a positive number).

It is easy to show that the *net irradiance*, $E_d - E_u$, *always decreases with depth in source-free water.* Integrating Gershun's law (5.37) from depth z_1 to z_2, where $z_1 < z_2$, gives

$$\int_{z_1}^{z_2} d(E_d - E_u) = -\int_{z_1}^{z_2} a(z)\, E_o(z)\, dz$$

$$(E_d - E_u)\big|_{z_2} - (E_d - E_u)\big|_{z_1} = -\int_{z_1}^{z_2} a(z)\, E_o(z)\, dz\,.$$

The right hand side of the last equation is always negative, which implies

$$(E_d - E_u)\big|_{z_1} \geq (E_d - E_u)\big|_{z_2}\,.$$

Approximate relations for R and K_d

Relations such as Eqs. (5.67) and (5.68) are exact in the absence of internal sources. A number of approximate relations among various IOP's and AOP's also have been developed over the years. These relations often are based on arguments drawn from radiative transfer theory combined with analysis of actual data or – more often – with numerical simulations substituting for real data.

Consider, for example, the irradiance reflectance just below the sea surface, $R(z=w=0) \equiv R(0)$. We can reason that $R(0)$ should be directly proportional to the backscattering coefficient b_b, which helps convert downwelling photons into upwelling photons, and inversely proportional to the absorption coefficient a, which denies photons the chance to be backscattered. We thus write

$$R(0) = \alpha\, \frac{b_b}{a}\,, \tag{5.73}$$

where the proportionality constant α depends on the radiance distribution, i.e. on the solar zenith angle, diffuse sky lighting, sea state, shape of the scattering phase function, and so on. Initial studies of Eq. (5.73) by Gordon, *et al.* (1975) and by Morel and Prieur (1977) showed that $\alpha \approx 0.33$ *for the sun at the zenith* and for a level sea surface. The resulting relation,

$$R(0) \approx 0.33 \, \frac{b_b}{a}, \tag{5.74}$$

is widely cited.

Kirk (1984) numerically studied the dependence of α on the solar angle and found

$$R(0) \approx \left(0.975 - 0.629\mu_{sw}\right)\frac{b_b}{a}. \tag{5.75}$$

Here μ_{sw} is the cosine of the nadir angle of the solar beam *after refraction through a level sea surface.* By Snell's law, Eq. (4.8),

$$\mu_{sw} = \cos\left[\sin^{-1}\left(\frac{1}{n_w}\sin\theta_s\right)\right], \tag{5.76}$$

where $n_w \approx 1.34$ is the index of refraction of the water and θ_s is the sun's zenith angle. In Eq. (5.75), μ_{sw} ranges from 1 for the sun at the zenith to $\mu_{sw} \approx 0.66$ for the sun at the horizon. Thus Kirk's α ranges from 0.35 to 0.56, depending on the solar zenith angle. Kirk used the Petzold turbid- harbor phase function seen in Fig. 3.13, and he assumed a level sea surface in his numerical studies.

More recent numerical simulations by Morel and Gentili (1991) led to

$$\begin{aligned} R(0) \approx \Big[&\left(0.6279 - 0.2227\eta_b - 0.0513\eta_b^2\right) \\ &+ \left(-0.3119 + 0.2465\eta_b\right)\mu_s \Big]\frac{b_b}{a}. \end{aligned} \tag{5.77}$$

Here η_b is the ratio of backscattering by water molecules to total backscattering, and $\mu_s = \cos\theta_s$. The parameter η_b depends on wavelength and on the nature of the particulate scattering; η_b ranges from near one in very clear waters at blue wavelengths to near zero at red wavelengths or in waters with high particle loads. The α values corresponding to Eq. (5.77) lie in the range 0.29 to 0.63; $\alpha = 0.32$ for $\eta_b = 0.5$ and $\mu_s = 1$.

Gordon (1989b) examined the dependence of $R(0)$ on the sea state and on the shape of the phase function. He found that the dependence of $R(0)$ on the solar angle θ_s is insensitive to the sea state for solar angles of less than 60°. On the other hand, the relation between $R(0)$ and θ_s does depend on the shape of $\tilde{\beta}(\psi)$ at large scattering angles ($\psi > 40°$). This is not surprising, because single scattering through large angles is the process primarily responsible for redirecting downwelling photons into upward directions.

Gordon (1992) also investigated the effects of vertical stratification on $R(0)$. He found that if the absorption and scattering coefficients covary with depth, then the reflectance of the stratified water is usually to within a few percent the same as the reflectance of a homogeneous water body whose a and b_b values are certain weighted depth averages of the actual $a(z)$ and $b_b(z)$ profiles. In such cases, the use of simple formulas like those above is justified. However, if a and b_b do not covary with depth, which is often the case (recall Fig. 3.22), then substantial errors (~20% or greater) in $R(0)$ result if the actual $a(z)$ and $b_b(z)$ profiles are replaced by depth-averaged values. In such cases, the prediction of $R(0)$ requires detailed calculations based on the RTE.

Thus over the years, the deceptively simple approximation $R(0) \approx 0.33b_b/a$ has been considerably refined. But still more work remains to be done, especially in regard to applying such equations to case 2 waters.

A similar story can be told regarding formulas relating K_d to a and b. One of the oldest such approximations is due to Honey [see Wilson (1979)]:

$$K_d \approx a + \frac{b}{6} = c - \frac{5}{6}b. \tag{5.78}$$

This formula can be in error by 30% or more, especially near the sea surface.

Equations (5.65) or (5.67) show that $K_d \approx a/\overline{\mu}_d$, to the extent that the diffuse backscattering and reflectance terms (which are usually small) can be ignored. This result explains the observed strong correlation between absorption and downwelling diffuse attenuation.

Numerical simulations by Kirk (1984) give

$$\overline{K}_d \approx \frac{a}{\mu_{sw}}\left[1 + \left(0.425\mu_{sw} - 0.19\right)\frac{b}{a}\right]^{1/2}, \tag{5.79}$$

where $\overline{K}_d$ is the average of $K_d(z)$ over the euphotic zone, and μ_{sw} is the cosine of the refracted solar angle, defined in Eq. (5.76). The simulations leading to Eq. (5.79) used the Petzold turbid-harbor phase function seen in Fig. 3.13. Extending the analysis to other VSF's gives (Kirk, 1991)

$$\overline{K}_d = \frac{a}{\mu_{sw}}\left[1 + G(\mu_{sw},g)\frac{b}{a}\right]^{1/2}, \tag{5.80}$$

where

$$G(\mu_{sw},g) = \mu_{sw}\left(\frac{2.236}{g} - 2.447\right) - \left(\frac{0.849}{g} - 0.739\right).$$

Here g is the mean cosine of the scattering angle ψ, defined as in Eq. (3.35). The function $G(\mu_{sw}, g)$ parameterizes the influence of the shape of the scattering phase function on $\bar{K}_d$

Approximate relation like Eqs. (5.79) and (5.80) are simple enough to be convenient and accurate enough to be useful, at least in homogeneous, case 1 waters. However, the user of such formulas must keep in mind that they are approximations and that reality can be more complicated than these equations imply.

5.13 Polarization

The *polarization* of light refers to the behavior of the plane of oscillation of the light's (or the photons') electric field vector. If all of the photons in a beam of light have their electric fields oscillating in the same fixed plane, the light is said to be linearly (or plane) polarized. If the plane of oscillation rotates, the light is either right or left circularly polarized (depending on the direction of rotation), or elliptically polarized. If the plane of oscillation changes randomly from one instant to the next (i.e. if the photons have randomly oriented electric field directions), the light is unpolarized. Partially polarized light can be viewed as a mixture of unpolarized and polarized light beams.

We can anticipate for three reasons that underwater light fields are partially polarized. First, sky light incident on the water surface is polarized to an extent that depends on atmospheric conditions (particles, cloudiness) and on the direction relative to the sun. Second, scattering of even unpolarized light by water molecules or by small particles generates partially polarized light. (This is the process by which unpolarized sunlight yields partially polarized sky light when unpolarized solar photons are scattered by air molecules.) And finally, the transmission of unpolarized sunlight through the sea surface (a dielectric interface) yields partially polarized light. The underwater environment is one of the few places in nature where unpolarized light (from the sun) is partially transformed into elliptically polarized light. Polarization of underwater light was first reported by Le Grand (1939); the first detailed measurements were made by Waterman (1954; see also Ivanoff, 1974).

Stokes vectors and Mueller matrices

The polarization state of a light field is usually specified by the four-component *Stokes vector* $\underline{S} = (I, Q, U, V)^{\mathrm{T}}$; here the superscript "T" denotes the transpose. The four components of $\underline{S}$, called the *Stokes parameters*, each have units of radiance and, like the unpolarized radiance $L(\vec{x};t;\hat{\xi};\lambda)$, each is a function of position, time, direction, and wavelength. Optics textbooks show how *I, Q, U*, and *V* can be measured by placing plane and circular polarizers *in front of the diffuser* in the instrument shown in Fig. 1.5 [see, for example, Bohren and Huffman (1983)].   The instrument of Fig. 1.5, without any polarizers, is measuring *I*, which is just the total radiance *L*. Parameters *Q, U*, and *V* are zero if the light field is unpolarized. Parameters *Q* and *U* are related to the state of *linear* polarization of the radiance, and *V* is related to the state of *circular* polarization.   In the most general case of partially polarized radiance, each of the Stokes parameters is non-zero. Although *Q, U*, and *V* have units of radiance, they can be positive or negative. For example, positive *V* corresponds by convention to right circular polarization and negative *V* corresponds to left circular polarization; *I* is always positive. In general $I^2 \geq Q^2 + U^2 + V^2$.

The definition of the Stokes parameters is not unique, and various linear combinations of *I, Q, U*, and *V* are often used to describe polarized light. For example, the classic treatise by Chandrasekhar (1960) uses $(I_{\parallel}, I_{\perp}, U, V)$ where $I_{\parallel} = \frac{1}{2}(I + Q)$ and $I_{\perp} = \frac{1}{2}(I - Q)$.

The quantity $\sqrt{(Q^2 + U^2 + V^2)}/I$ is called the *degree of polarization*; it ranges from zero for unpolarized light to one for complete polarization. The quantity $\sqrt{(Q^2 + U^2)}/I$ is the degree of *linear* polarization, and *V/I* is the degree of *circular* polarization.

In a given scattering event, the light described by an incident Stokes vector $\underline{S}'(\hat{\xi}';\lambda')$ is scattered into $\underline{S}(\hat{\xi};\lambda)$, which in general describes radiance of a different direction, wavelength, and state of polarization. The most general linear transformation of a four-component Stokes vector can be represented by a four-by-four matrix $\underline{P}$, called the *phase*, or *scattering matrix*. Its sixteen elements specify how the scattering process changes the light field. Writing out the matrix equation $\underline{S} = \underline{P}\underline{S}'$ gives

$$
\begin{pmatrix} I \\ Q \\ U \\ V \end{pmatrix} = \begin{pmatrix} p_{11} & p_{12} & p_{13} & p_{14} \\ p_{21} & p_{22} & p_{23} & p_{24} \\ p_{31} & p_{32} & p_{33} & p_{34} \\ p_{41} & p_{42} & p_{43} & p_{44} \end{pmatrix} \begin{pmatrix} I' \\ Q' \\ U' \\ V' \end{pmatrix} .
\tag{5.81}
$$

Each element p_{ij} of the phase matrix is in essence a volume scattering function that operates on a particular component of the incident Stokes vector $\underline{S}'$ to transform it into a component of the final $\underline{S}$. From Eq. (5.81) we see that p_{11} transforms unpolarized radiance $I'(\hat{\xi}';\lambda')$ into unpolarized radiance $I(\hat{\xi};\lambda)$; hence p_{11} is just the phase function as we have previously defined it. Likewise, p_{41} transforms unpolarized radiance I' into circularly polarized radiance V; p_{44} carries circularly polarized radiance V' into circularly polarized radiance V, and so on.

A subtlety in Eq. (5.81) must now be addressed. By convention, the incident Stokes vector $\underline{S}'$ is defined by measurements made in the plane determined by directions $\hat{\xi}'$ and $\hat{i}_3$; this plane is called the *incident meridian plane*. The final, or scattered, Stokes vector $\underline{S}$ is measured in the plane determined by directions $\hat{\xi}$ and $\hat{i}_3$; this is the *final meridian plane*. The scattering properties of the water are most conveniently described with reference to the plane determined by $\hat{\xi}'$ and $\hat{\xi}$; this is the *scattering plane*, in which the scattering angle is $\psi = \cos^{-1}(\hat{\xi}'{\cdot}\hat{\xi})$. It is thus common practice to decompose $\underline{S} = \underline{P}\,\underline{S}'$ into

$$
\underline{S} = \underline{R}_2\,\underline{M}\,\underline{R}_1\,\underline{S}' .
\tag{5.82}
$$

Here $\underline{R}_1$ is a 4×4 matrix that rotates the vector $\underline{S}'$ from the incident meridian plane into the scattering plane. Matrix $\underline{M}$, called the *Mueller matrix*, is the 4×4 matrix that *describes the scattering process relative to the scattering plane*. Vector $\underline{R}_1\underline{S}'$ is in the scattering plane, and can be operated upon by $\underline{M}$. The resulting vector $\underline{M}\,\underline{R}_1\,\underline{S}'$, which is still in the scattering plane, must then be rotated by the 4×4 matrix $\underline{R}_2$ from the scattering plane into the final meridian plane, in which $\underline{S}$ is defined. The forms of the rotation matrices $\underline{R}_1$ and $\underline{R}_2$ appropriate for the [*I, Q, U, V*] form of the Stoke's vector, and figures necessary for visualizing this entire process, are given in Kattawar (1994). Chandrasekhar (1960) uses different $\underline{R}_1$ and $\underline{R}_2$, because he uses the [$I_\parallel$, $I_\perp$, *U, V*] representation of $\underline{S}$, mentioned above.

The decomposition (5.82) thus separates the scattering properties of the medium, which are completely described by $\underline{M}$, from the bookkeeping related to the different coordinate systems. Such transformations were not

required in our previous discussions because unpolarized radiance L is a scalar, and is therefore independent of coordinate systems.

Optics textbooks [e.g. Bohren and Huffman (1983); see also Anderson (1992)] explain in detail how the elements m_{ij} of the Mueller matrix $\underline{M}$ can be measured by placing various combinations of linear and circular polarizers in the incident and scattered beams of the instrument shown in Fig. 5.1. The instrument of Fig. 5.1, shown without polarizers, is measuring m_{11}.

In general, each of the elements m_{ij} of the Mueller matrix can be non-zero and independent of the other elements, although certain inequalities can be established between the elements (Fry and Kattawar, 1981). However, any *symmetries* in the scattering medium result in simplifications in the form of the Mueller matrix. In particular, if the scattering medium consists of a collection of spherically symmetric particles of various sizes, or if the medium contains equal numbers of nonspherical particles and their mirror images in random orientations, then $\underline{M}$ has the form

$$\begin{pmatrix} m_{11} & m_{12} & 0 & 0 \\ m_{12} & m_{11} & 0 & 0 \\ 0 & 0 & m_{33} & m_{34} \\ 0 & 0 & -m_{34} & m_{33} \end{pmatrix}.$$

If the spherical particles are small enough to be treated by Rayleigh scattering theory, then $m_{34} = 0$. Indeed, the Mueller matrix for Rayleigh scattering is

$$\underline{M}_{\text{Ray}} = \frac{3}{16\pi} \begin{pmatrix} 1 + \cos^2\psi & -\sin^2\psi & 0 & 0 \\ -\sin^2\psi & 1 + \cos^2\psi & 0 & 0 \\ 0 & 0 & 2\cos\psi & 0 \\ 0 & 0 & 0 & 2\cos\psi \end{pmatrix}, \tag{5.83}$$

where ψ is the scattering angle. Note that m_{11} in Eq. (5.83) is just the Rayleigh phase function, as can be obtained from Eq. (3.29).

In presenting Mueller matrices, it is customary to divide each element m_{ij} by m_{11}, which is never zero, and to ignore the normalizing factor. All matrix elements then lie in the interval -1 to $+1$. This normalization by m_{11} emphasizes the polarization effects of the scattering process, rather than the angular nature of the scattering, which is contained in m_{11}. This *reduced form* of Eq. (5.83) then reads

$$
\underline{M}_{\text{Ray}} =
\begin{pmatrix}
1 & -\dfrac{\sin^2\psi}{1 + \cos^2\psi} & 0 & 0 \\[2ex]
-\dfrac{\sin^2\psi}{1 + \cos^2\psi} & 1 & 0 & 0 \\[2ex]
0 & 0 & \dfrac{2\cos\psi}{1 + \cos^2\psi} & 0 \\[2ex]
0 & 0 & 0 & \dfrac{2\cos\psi}{1 + \cos^2\psi}
\end{pmatrix} . \tag{5.84}
$$

The scattering-angle dependence of the reduced $\underline{M}$ often is displayed as a four-by-four panel of figures, each of which shows ψ along the abscissa. The graphical representation of Eq. (5.84) is shown in Fig. 5.6(a).

Voss and Fry (1984) measured reduced Mueller matrices at $\lambda = 488$ nm in a variety of ocean waters; one such measurement from high-chlorophyll Atlantic waters is shown in Fig. 5.6(b). Although the ocean water reduced $\underline{M}$ is similar to the reduced $\underline{M}_{\text{Ray}}$, the differences are significant. The fact that the normalized ocean m_{12} and m_{21} do not reach -1 at $\psi = 90°$ can be traced in part to the 0.835 factor in Eq. (3.28). The deviation of m_{22} from 1 indicates the presence of nonspherical particles in the water. Note also that m_{33} and m_{44} are significantly greater than zero at $\psi = 90°$; Voss and Fry associated this behavior with the phytoplankton. Measurements of m_{33} and m_{44} at the same location but taken near the bottom, where there was resuspended sediment and detritus but few phytoplankton, showed m_{33} and m_{44} to be zero at $\psi = 90°$.

Quinby-Hunt, *et al.* (1989) measured non-zero m_{34} elements in certain phytoplankton. They were able to explain this behavior by modeling the phytoplankton cells as coated spheres: a cell core with complex index of refraction $n - ik = 1.08 - i0.05$, plus a thin cell wall with $n - ik = 1.13 - i0.04$. Lofftus, *et al.* (1992) measured small, but nonzero, m_{14} values for suspensions of a certain dinoflagellate. Recall that m_{14} depolarizes circularly polarized light. This optical activity appears to be associated with the large helical chromosomes in the phytoplankton cells. High concentrations of these phytoplankton in oceanic waters would result in nonzero m_{34} or m_{14} values. Such studies illustrate the utility of Mueller matrix measurements as a tool for extracting information about the scattering particles.

Stokes vectors and Mueller matrices are discussed in detail, starting with Maxwell's equations, in Kattawar (1994).
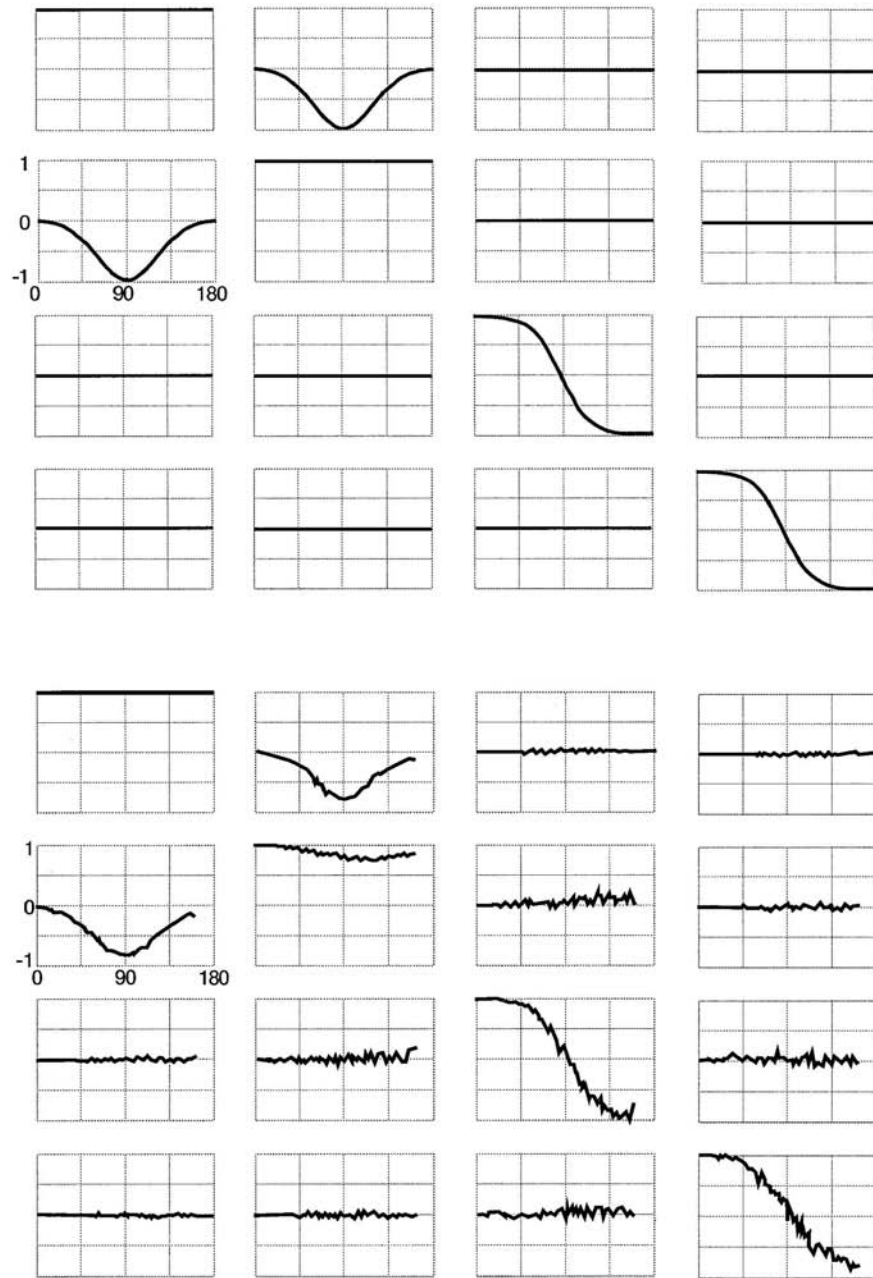
Fig. 5.6. Graphical display of a reduced Mueller matrix. The upper panel shows the Mueller matrix for Rayleigh scattering, Eq. (5.89). The lower panel shows a Mueller matrix measured in the Atlantic Ocean. [reproduced from Voss and Fry (1984), by permission]

Polarized radiance transfer

One of the beauties of the Stokes vector–Mueller matrix description of polarized light is that the radiance transfer equation has the same *form* for polarized radiance as for unpolarized radiance. In essence, it is necessary only to replace L by $\underline{S}$ and the VSF β by the phase matrix $\underline{P}$. Equation (5.23) recast for polarized radiance is then

$$\mu \frac{d\underline{S}(\hat{\xi})}{dz} = -c\,\underline{S}(\hat{\xi}) + \int_{\Xi} \underline{P}(\hat{\xi}' \to \hat{\xi})\,\underline{S}'(\hat{\xi}')\,d\Omega(\hat{\xi}') + \underline{Source}(\hat{\xi})\,, \qquad (5.85)$$

Using Eq. (5.82), the integral term in Eq. (5.85) can be written as

$$\int_{\Xi} \underline{R}_2(\hat{\xi})\,\underline{M}(\hat{\xi}' \to \hat{\xi})\,\underline{R}_1(\hat{\xi}')\,\underline{S}'(\hat{\xi}')\,d\Omega(\hat{\xi}')$$

to show the Mueller matrix explicitly. The source term in Eq. (5.85) must of course be tailored to give the Stokes vector of any internal light sources. Other equations associated with the solution of Eq. (5.85), in particular the boundary conditions expressed by Eqs. (4.3) and (4.4), must also be elevated from the scalar to the vector level. Quantities such as the Fresnel reflectance of the water surface, shown in Fig. 4.3, also must be revised to take into account the dependence of reflection and refraction on polarization; see for example Kattawar and Adams (1989).

The polarization of sky light has been studied for almost two centuries and vector, or polarized, radiance computations based on Eq. (5.85) are routinely performed in atmospheric optics studies. However, little attention has been paid to polarization in the underwater environment. This is partly because of instrumental and computational difficulties and partly for scientific reasons. It is difficult enough to measure a scalar radiance distribution $L(\hat{\xi};\lambda)$, $\hat{\xi} \in \Xi$, under water; the additional measurements required to determine the full Stokes vector are seldom made. Moreover, in order to predict how a given water body will scatter polarized light, we must know the Mueller matrix. With the exception of the previously cited measurements made by Voss and Fry (1984), little information is available on oceanic $\underline{M}$ values. There is no systematic body of knowledge concerning how the matrix elements depend on the highly variable constituents of natural waters. Even though the functional form of the RTE is the same for the vector and scalar cases, considerably more programming effort and computer time are required to solve Eq. (5.85), as opposed to Eq. (5.23). And finally, many of the processes of interest to oceanographers and

limnologists, such as photosynthesis and heating, are assumed to be independent of the polarization state of the light field. Thus there is little incentive to measure polarization or to incorporate it into predictive numerical models.

However, predictive numerical models for polarized underwater radiance distributions do exist (Kattawar and Adams, 1989). Numerical simulations (Adams and Kattawar, 1993) with these models indicate that the difference in L (computed from the scalar RTE) and the I component of the Stokes vector (computed from the vector RTE) is usually 5% to 10%, but can exceed 15% under some conditions. The difference in L and I depends on direction, depth, solar angle, and single-scattering albedo. The difference $I - L$ is both positive and negative (depending on the direction), so that the *irradiances* computed from scalar and vector theory are nearly identical. Processes such as heating and photosynthesis, which depend on the total scalar irradiance E_o, should therefore be equally well modeled using vector or scalar theory. Although *in principle we will always get a wrong answer if we use the scalar RTE* (5.23) *instead of the vector RTE* (5.85), the answer will seldom be wrong by much. Other sources of error, such as uncertainties in the IOP's or in the boundary values, generally will be the main source of error in computed underwater radiances. In some problems however, especially those involving remote sensing or lasers, the state of polarization may be an essential part of the solution; in such cases we *must* work with Eq. (5.85).

We shall for the most part neglect polarization in our subsequent discussions. The development of radiative transfer theory is difficult enough at the scalar level; the mathematical complications associated with carrying along the vector notation would not be repaid by a corresponding increase in our understanding of underwater optics.

We do wish to note, however, that polarization does have some interesting physical and biological consequences. Clever use of circularly polarized artificial light to improve underwater visibility can be traced back to Gilbert and Pernicka (1966). Extensive investigations by Waterman and others [Waterman (1988), and references therein] have shown that marine organisms ranging from plankton to fish use polarization as an aid for orientation, and possibly for navigation. Finally, polarization of sunlight reflected by the sea surface is routinely used to extract information in remote sensing studies.

5.14 Raman Scattering

Starting around 1980, oceanographers began routinely making measurements of spectral irradiances in a variety of waters. These measurements were used to compute diffuse attenuation functions, $K_d(z;\lambda)$ and $K_u(z;\lambda)$, or to recover absorption coefficients $a(z;\lambda)$ via Gershun's law, Eq. (5.37). However, anomalous behavior was noted in these quantities at yellowish-green to red wavelengths ($\lambda > 550$ nm), at depths below a few tens of meters. The computed K-functions and absorption coefficients were often less than the accepted values for pure water [see, for example, Spitzer and Wernand (1981), and Sugihara, *et al.*, (1984)]. These mysterious results were sometimes attributed to imperfect instrumentation.

If there is an internal source of light at the wavelength of interest, then it will appear that less energy is being absorbed at that wavelength, and hence the absorption coefficient as recovered by Gershun's law will be less than the value of the true absorption coefficient obtained in the source-free case. Similarly, the presence of additional light from an internal source means that the irradiances decrease less quickly with depth, and thus the K-functions are less than they would be without the source.

Chlorophyll fluoresces strongly in a wavelength band centered at about $\lambda = 685$ nm, as will be seen in Section 5.15. Thus sunlight-induced fluorescence can explain the anomalous measurements near 685 nm, in waters containing phytoplankton. However, the chlorophyll fluorescence band is only about 25 nm wide, and so chlorophyll fluorescence cannot serve as an internal source in the wavelength region between 550 nm and 650 nm. Moreover, the anomalous behavior was observed in even the clearest waters, where fluorescence by chlorophyll or other substances was negligible.

Sugihara, *et al.* (1984) recognized that *Raman scattering* by the water molecules themselves provides a mechanism for scattering light inelastically from shorter to longer wavelengths, as is needed to explain the observations.

A rough visualization of Raman scattering can be obtained by thinking of the electron cloud of a molecule, which is vibrating at the molecular vibrational frequencies. The oscillating electric field of the incident electromagnetic wave (photon) causes the molecule's electron cloud to oscillate also at the photon's frequency. The Raman effect occurs when the molecule re-radiates at the sum and difference frequencies. (If the molecule is already in an excited state – and some always are at any temperature above absolute zero – then the molecule may emit a photon of *shorter* wavelength than the incident photon, and thereby return to the ground state. However, at the temperatures of liquid water, Raman scattering from longer to shorter

wavelengths is insignificant.) Raman scattering occurs in solids, liquids, and gasses.

The energy of the scattered photon equals the energy of the incident photon plus or minus a vibrational or rotational energy difference of the molecule. Because these energy differences are determined by the molecule's structure, Raman scattering was recognized as a powerful tool for probing molecular structure, long before its oceanographic significance was realized. The above observations imply that the incident and scattered light are related by a *frequency* shift that depends on the molecule.   The corresponding *wavelength* shift between the incident and scattered light also depends on the incident wavelength, as we shall see below.

In order to incorporate Raman scattering into the radiance transfer equation (5.20), we must develop an appropriate volume inelastic scattering function $\beta^R(\hat{\xi}' \to \hat{\xi}; \lambda' \to \lambda)$. The Raman β^R is a specific instance of the β^I seen in Eq. (5.10). This development has been done with great care by Haltrin and Kattawar (1991, 1993).   The following discussion recapitulates their formulation, with minor changes as required to fit the notation and terminology of Section 5.3. They show that the spectral volume inelastic scattering function appropriate for Raman scattering, β^R, has the form of Eq. (5.12), namely

$$\beta^R(\hat{\xi}' \to \hat{\xi}; \lambda' \to \lambda) \;=\; b^R(\lambda' \to \lambda)\, \tilde{\beta}^R(\hat{\xi}' \to \hat{\xi}) \quad (\mathrm{m^{-1}\ sr^{-1}\ nm^{-1}}) . \qquad (5.86)$$

Here b^R is the volume *Raman scattering coefficient*, with units of $\mathrm{m^{-1}\ nm^{-1}}$; and $\tilde{\beta}^R$ is the *Raman scattering phase function*, with units of $\mathrm{sr^{-1}}$. Just as with elastic scattering, the phase function gives the directional distribution of the Raman scattered radiance. The Raman total scattering coefficient can be dissected to give

$$b^R(\lambda' \to \lambda) \;=\; a^R(\lambda')\, f^R(\lambda' \to \lambda) \qquad (\mathrm{m^{-1}\ nm^{-1}}) , \qquad (5.87)$$

where

$$a^R(\lambda') \;\equiv\; \int_{\lambda'}^{\infty} b^R(\lambda' \to \lambda)\, d\lambda \qquad (\mathrm{m^{-1}}) \qquad (5.88)$$

is the *Raman absorption coefficient* [recall Eq. (5.13)]. For applications to hydrologic optics, the integral in Eq. (5.88) is taken over wavelengths $\lambda > \lambda'$, since only Raman scattering to longer wavelengths is significant. Recall that $a^R(\lambda')$ is a measure of how strongly radiance is "absorbed" at wavelength λ', i.e. is inelasticly scattered to longer wavelengths. The value of $a^R(\lambda')$ is included in the beam attenuation coefficient $c(\lambda')$, as shown in Eq. (5.15).

   The factor $f^R(\lambda' \to \lambda)$ is the *Raman wavelength redistribution function*, with units of nm^{-1}. This function specifies the wavelength λ where radiance of wavelength λ' ends up after being Raman scattered. We now consider each of the functions a^R, $\tilde{\beta}^R$, and f^R in turn.

   Note first that in the literature, our $a^R(\lambda')$ is usually called the "Raman scattering coefficient." We reserve this name for $b^R(\lambda' \to \lambda)$. If the Raman scattering cross section (as defined by spectroscopists, with units of m^2 per molecule) is formulated so as to relate the incident and scattered *powers* (in watts), then the wavelength dependence for non-resonant Raman scattering (scattering in which the frequency of the incident photon is not near a resonance frequency of the molecule) is (scattered wavelength)$^{-4}$. If the formulation is in terms of the *numbers* of incident and scattered photons, the dependence is (incident wavelength)$^{-1}$ × (scattered wavelength)$^{-3}$. This last form arises from an additional factor of (scattered wavelength)/(incident wavelength) that is required to convert power to number of photons (recall Eq. 1.1). These matters are discussed in detail by Desiderio (2000), who does an excellent job of clarifying the confusion in some previous oceanographic literature about the wavelength dependence of Raman scattering. Thus we can write

$$a^R(\lambda) = a_o^R \left(\frac{\lambda_o}{\lambda} \right)^4 , \tag{5.89}$$

which is appropriate for radiative transfer calculations in terms of power (i.e., for radiance predictions).

   a_o^R, the value of a^R at some reference wavelength λ_o, is often given at 488 nm. A factor-of-five range in values of a_o^R can be found in the oceanographic literature. However, the earlier, larger values for a_o^R [in particular the often-cited value of $a_o^R = 3.2 \times 10^{-3}\ m^{-1}$ corresponding to the data of Slusher and Derr (1975)] are almost certainly incorrect. Measurements by Marshall and Smith (1990) yielded $a^R(488\ nm) = 2.6 \times 10^{-4}\ m^{-1}$, and the more recent paper by Desiderio (2000) gives $a^R(488\ nm) = 2.4 \times 10^{-4}\ m^{-1}$. Comparisons of numerical-model output and oceanic irradiance measurements by Kattawar and Xu (1992) also imply the correctness of a "small" value for a_o^R. Regardless of its exact value, we note that a^R is roughly one tenth the magnitude of the scattering coefficient of pure water, b_{sw}, as seen in Table 3.5. Thus roughly one in ten photons scattered *by water molecules* is Raman-scattered to another wavelength.

   The Raman scattering phase function $\tilde{\beta}^R(\hat{\xi}' \to \hat{\xi}) = \tilde{\beta}^R(\psi)$, where ψ is the scattering angle, can be written as

$$\tilde{\beta}^R(\psi) \;=\; \frac{3}{16\pi}\,\frac{1+3\rho}{1+2\rho}\left[\,1\;+\;\left(\frac{1-\rho}{1+3\rho}\right)\cos^2\psi\,\right] \qquad (\mathrm{sr}^{-1})\,, \qquad (5.90)$$

where ρ is a parameter called the depolarization ratio. This quantity depends on the wavenumber shift κ'' (defined below). The average value of ρ for Raman scattering in water is near 0.17 [see Ge., *et al.*, (1993), their Fig. 2], in which case Eq. (5.90) reduces to

$$\tilde{\beta}^R(\psi) \;=\; 0.067\,(\,1\;+\;0.55\cos^2\psi) \qquad (\mathrm{sr}^{-1})\,. \qquad (5.91)$$

This phase function is very similar to that for pure sea water, Eq. (3.30). Note that the $\tilde{\beta}^R$ of Eq. (5.91) satisfies the normalization condition (3.8).

We warn the reader that the literature contains equivalent, but superficially different, representations of $\tilde{\beta}^R$. For example, Marshall and Smith (1990) show a form [their Eq. (6); see also Kattawar and Xu (1992)] involving $\sin^2\vartheta$, where ϑ is the angle between the polarization vector of the incident plane-polarized light and the direction of the scattered light; this form was convenient for their experimental arrangement. As for all scattering processes, Raman-scattered light is partially polarized even if the incident radiance is unpolarized. However, we shall not consider the polarization aspects of Raman scattering, which are discussed in Kattawar and Xu (1992).

The Raman wavelength redistribution function $f^R(\lambda'\!\to\!\lambda)$ is most conveniently described in terms of the corresponding *wavenumber redistribution function* $f^R(\kappa'')$, where κ'' is the *wavenumber shift*, expressed in units of cm^{-1}. This follows because the Raman-scattered light undergoes a *frequency* shift that is independent of the incident frequency. The wavenumber κ in cm^{-1} is related to the wavelength λ in nm by $\kappa = 10^7/\lambda$, and to the frequency ν by $\kappa = \nu/c$, where c is the speed of light.

According to Walrafen (1967), the shape of $f^R(\kappa'')$ for water is given by a sum of four Gaussian functions:

$$f^R(\kappa'') \;=\; \left[\left(\frac{\pi}{4\ln2}\right)^{\!\frac{1}{2}}\sum_{i=1}^{4}A_i\right]^{-1}\sum_{j=1}^{4}A_j\,\frac{1}{\Delta\kappa_j}\exp\!\left[-4\ln2\,\frac{(\kappa''-\kappa_j)^2}{\Delta\kappa_j^2}\right] \qquad (\mathrm{cm})\,, \qquad (5.92)$$

where

$\kappa'' =$ the wavenumber shift of the Raman-scattered light, *relative to the wavenumber κ' of the incident light*;

$\kappa_j =$ the center of the jth Gaussian function, in cm^{-1};

$\Delta\kappa_j =$ the full width at half maximum of the jth Gaussian function, in cm^{-1}; and

$A_j =$ the nondimensional weight of the jth Gaussian function.

The values of A_j, κ_j, and $\Delta\kappa_j$ for pure water at a temperature of 25° C are given in Tab. 5.3.

The function $f^R(\kappa'')$ can be interpreted as a probability density function giving the probability that a photon of any incident wavenumber $\kappa' = 10^7/\lambda'$, if Raman scattered, will be scattered to a wavenumber

$$\kappa = \kappa' - \kappa''.$$

Consider, for example, a photon with $\lambda' = 500$ nm, which corresponds to $\kappa' = 20{,}000$ cm^{-1}. Quick inspection of Tab 5.3 shows that this photon is most likely to be shifted by roughly 3,500 cm^{-1} to $\kappa = 16{,}500$ cm^{-1}, which corresponds to $\lambda = 600$ nm.

The wavenumber function $f^R(\kappa'')$ satisfies the normalization

$$\int_0^{\kappa'} f^R(\kappa'') \, d\kappa'' = 1, \tag{5.93}$$

as is required of any probability distribution function. A change of variables from κ'' to λ in Eq. (5.93) leads us to the corresponding *wavelength* redistribution function $f^R(\lambda' \to \lambda)$. First note that if the water molecule absorbs no energy, the shift κ'' is zero, i.e., we have elastic scattering and $\lambda = \lambda'$. If the water molecule absorbs all of the incident photon's energy, then the emitted photon has $\lambda = \infty$, i.e., $\kappa = 0$ and so $\kappa'' = \kappa'$. Thus

$$\int_0^{\kappa'} f^R(\kappa'') \, d\kappa'' = \int_{\lambda'}^\infty f^R\left(\frac{10^7}{\lambda''}\right) \frac{d\kappa''}{d\lambda} \, d\lambda = \int_{\lambda'}^\infty f^R\left(\frac{10^7}{\lambda''}\right) \frac{10^7}{(\lambda)^2} \, d\lambda$$

$$\equiv \int_0^\infty f^R(\lambda' \to \lambda) \, d\lambda = \int_{\lambda'}^\infty f^R(\lambda' \to \lambda) \, d\lambda = 1.$$

In the last equation, we have identified the function

$$f^R(\lambda' \to \lambda) \equiv \begin{cases} \dfrac{10^7}{(\lambda)^2} f^R\left(\dfrac{10^7}{\lambda''}\right) = \dfrac{10^7}{(\lambda)^2} f^R\left[10^7\left(\dfrac{1}{\lambda'} - \dfrac{1}{\lambda}\right)\right] & \text{if } \lambda' < \lambda, \\[4mm] 0 & \text{if } \lambda' \geq \lambda, \end{cases} \tag{5.94}$$

as being the desired Raman wavelength redistribution function, with units of nm^{-1}. Note that the wavelengths must be given in nm, because of the factors of 10^7. This function is plotted in Fig. 5.7 for several values of λ'.

Table 5.3. Parameter values[a] for the Raman wavenumber
redistribution function $f^R(\kappa'')$ of Eq. (5.92),
for pure water at a temperature of 25° C.

j	A_j	κ_j (cm^{-1})	$\Delta\kappa_j$ (cm^{-1})
1	0.41	3250	210
2	0.39	3425	175
3	0.10	3530	140
4	0.10	3625	140

a. Data from Walrafen (1969), reproduced
by permission.
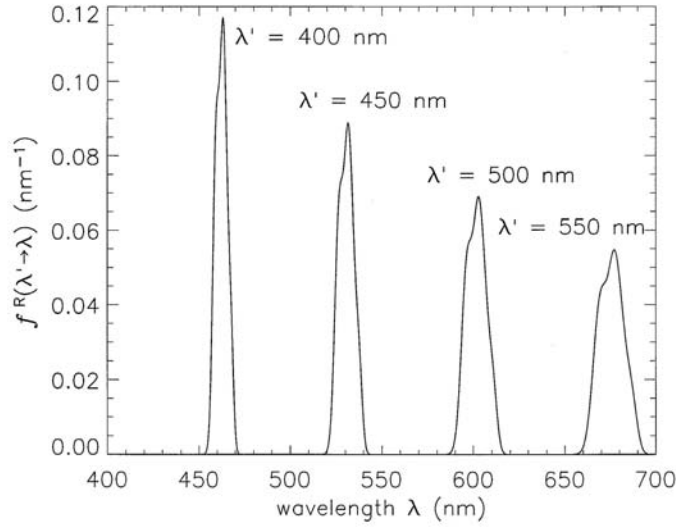
Fig. 5.7. The Raman wavelength redistribution function $f^R(\lambda' \to \lambda)$ of Eq. (5.94), for selected incident wavelengths λ'.

Equations (5.89), (5.91), (5.92) and (5.94) give us all of the pieces necessary to construct the volume inelastic scattering function for Raman scattering, $\beta^R(\hat{\xi}' \to \hat{\xi} ; \lambda' \to \lambda)$, as shown in Eqs. (5.86) and (5.87).

Since this is our first encounter with a specific inelastic scattering process, it is worthwhile to show explicitly the form of the RTE when Raman scattering is included:

$$\mu \frac{dL(z;\hat{\xi};\lambda)}{dz} = -c(z;\lambda) L(z;\hat{\xi};\lambda)$$

$$+ \int_{\Xi} \beta(z;\hat{\xi}'\rightarrow\hat{\xi};\lambda) L(z;\hat{\xi}';\lambda) d\Omega(\hat{\xi}')$$

$$+ \int_{0}^{\lambda}\int_{\Xi} \beta^{R}(\hat{\xi}'\rightarrow\hat{\xi};\lambda'\rightarrow\lambda) L(z;\hat{\xi}';\lambda') d\Omega(\hat{\xi}') d\lambda' . \tag{5.95}$$

This equation is an example of Eqs. (5.20) and (5.22). Recall that the $-cL$ term accounts for loss of radiance by Raman scattering to wavelengths greater than λ, whereas the term involving β^{R} accounts for the gain of radiance at λ from shorter wavelengths. The last term on the right hand side of Eq. (5.95) is thus an effective source term at wavelength λ; its evaluation clearly requires that the radiance be known at all wavelengths λ' less than λ, for which $\beta^{R} \neq 0$. Thus in order to solve Eq. (5.95) for the radiance at wavelength λ, we must work our way through a sequence of solutions of the RTE, beginning at some wavelength λ_1', for which there is no Raman scattering input from wavelengths less than λ_1'.

Figure 5.7 explains qualitatively how Raman scattering can explain the anomalous absorption and diffuse attenuation values mentioned at the beginning of this section. At wavelengths greater than roughly 550 nm, almost none of the solar radiation incident on the sea surface reaches depths of more than a few tens of meters, because of the high absorption by water itself. However, solar radiation at wavelengths less than 550 nm can penetrate to great depth. Part of the blue to green solar radiation at depth is Raman scattered into yellow to red wavelengths, as indicated in Fig. 5.7. This inelastic scattering process thereby provides an internal source of nonsolar photons, which are detected in irradiance measurements at long wavelengths. The Raman scattering process of course operates at all depths and wavelengths, but the inelasticly scattered light is usually negligible compared to the ambient solar light at shallow depths and at blue to green wavelengths. An instance when Raman scattering can be important at short wavelengths is seen in the filling of Fraunhofer lines in the solar spectrum; this is discussed in Kattawar and Xu (1992) and in Ge, *et al.* (1993).

Note also that because the phase function $\tilde{\beta}^{R}$ is symmetric about $\psi = 90°$, the downwelling solar photons will be Raman scattered almost equally into upwelling and downwelling directions. On the other hand, elastic backscattering is much weaker than elastic forward scattering; thus

E_u is much less than E_d. The Raman contribution to E_u will therefore be relatively much greater than the Raman contribution to E_d. We therefore expect K_u to be more sensitive than K_d to the effects of Raman-scattered light. This reasoning is consistent with observation; see, for example, Marshall and Smith (1990).

The same reasoning implies that the irradiance reflectance $R = E_u/E_d$ should increase with depth owing to Raman scattering. This behavior is seen in striking fashion in Fig. 5.8. The light line in the figure shows $R(z;\lambda=589$ nm) as measured in the very clear waters of the Sargasso Sea. $R(z;589)$ increases from near zero just below the surface to greater than 0.3 as depths below 100 m. (The large fluctuations in R below 120 m are intrumental noise at low light levels.) The heavy line in Fig. 5.8 shows
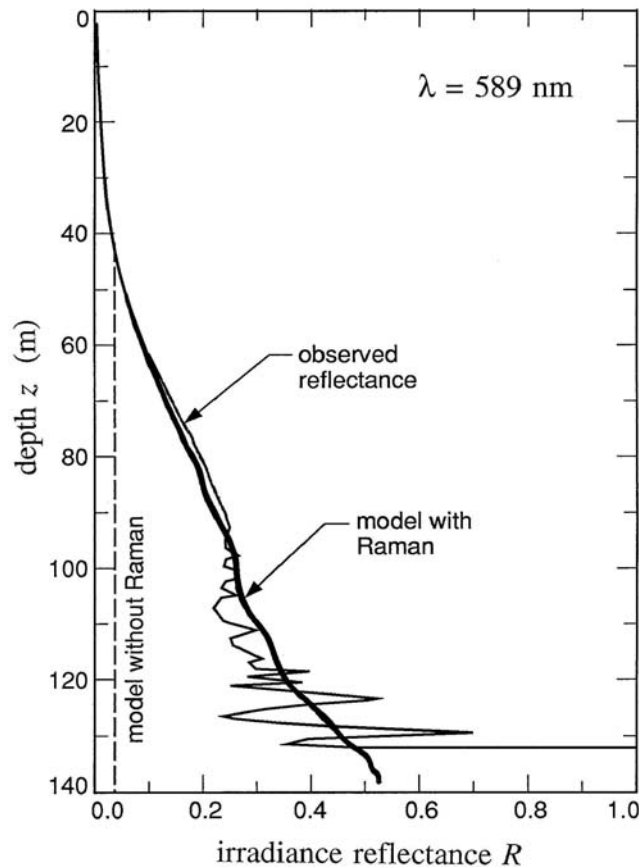
Fig. 5.8. Measured values of the irradiance reflectance $R = E_u/E_d$ at 589 nm in very clear water (light line), and predicted values with (heavy line) and without (dashed line) Raman scattering. [redrawn from Marshall and Smith (1990), by permission]

$R(z;589)$ as predicted by the model of Marshall and Smith (1990), which includes Raman scattering. The agreement between prediction and observation is excellent. However, if Raman scattering is omitted from their model, the predicted value of R remains at about 0.04; this behavior is shown by the dotted line in Fig. 5.8.

Equation (5.89) shows that the loss of energy from the incident-wavelength light field by Raman scattering is almost negligible compared to the loss by true absorption. Even at $\lambda' = 400$ nm, where the Raman absorption coefficient $a^R(\lambda')$ is largest and the true absorption coefficient of pure water $a_w(\lambda')$ is the smallest, the ratio a^R/a_w is less than 0.04.

In addition to the papers already cited, important studies of Raman-scattering effects on underwater light fields are found in Stavn and Weidemann (1988, 1992). We note in closing that the coefficients A_j, κ_j, and $\Delta\kappa_j$ seen in Eq. (5.92) depend weakly on temperature. As a consequence, the shapes of the wavelength redistribution functions seen in Fig. 5.7 vary slightly with the water temperature. This change of shape can be exploited as a way of remotely sensing water temperature; literature on this topic can be traced by beginning with Leonard and Sweeney (1988) and Collins, *et al.* (1984).

5.15 Fluorescence

Another inelastic process of considerable significance in natural waters is *fluorescence.* Fluorescence occurs when a molecule absorbs an incident photon and shortly thereafter emits a photon of greater wavelength. This process requires a rather long time from the viewpoint of a molecular physicist, 10^{-11} s to 10^{-8} s. Many researchers therefore view fluorescence as an absorption followed by an emission, rather than as a nearly instantaneous scattering process. These viewpoints have influenced the terminology. In fluorescence studies, λ' and λ are respectively called the *excitation* and *emission* wavelengths, rather than the incident and scattered wavelengths. However, for optical oceanographers, such distinctions between the fluorescence and the Raman scattering processes are somewhat irrelevant. The net result of Raman scattering and fluorescence is much the same: light is quickly transferred from shorter to longer wavelengths. Moreover, the most convenient way to include fluorescence in the radiance transfer equation is to use the same mathematical formalism as was developed for

the description of Raman scattering.   For consistency with our previous notation, we shall continue to use λ' and λ, rather than λ_{ex} (for λ') and λ_{em} (for λ), which are commonly seen in the literature on fluorescence.

   Many substances found in natural waters fluoresce. The most studied of these is chlorophyll. Other pigments found in living phytoplankton also fluoresce, as do many of the compounds found in yellow matter. Hydrocarbons and other pollutants often show strong fluorescence, especially when excited by ultraviolet light at wavelengths from 300 nm to 400 nm.
   Figure 5.9 illustrates the nature of fluorescence in natural waters. In panel (a), the excitation wavelength is $\lambda_{ex} \equiv \lambda' = 308$ nm. The peak
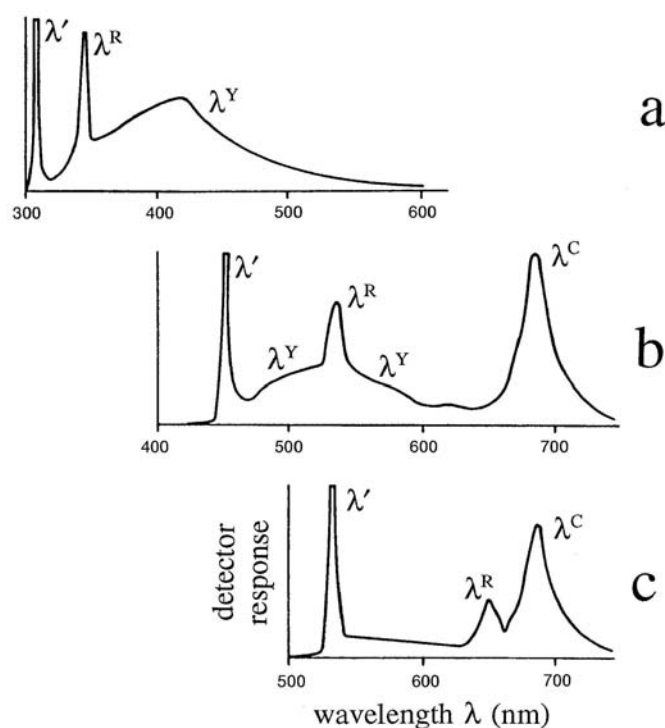
Fig. 5.9. Response of a water sample from the North Sea to excitation at three different wavelengths, λ'.   The symbol λ^R identifies the Raman band, λ^Y fluorescence by yellow matter, and λ^C fluorescence by chlorophyll. [redrawn from Diebel-Langohr, *et al*. (1986), by permission]

centered at $\lambda_{em} \equiv \lambda = 344$ nm is due to Raman scattering by the water itself. The broad fluorescence between 308 and ~600 nm, which peaks at blue wavelengths, is due to yellow matter (CDOM). Figure 5.9(b) shows the same water excited at $\lambda' = 450$ nm. As before, there is a relatively narrow Raman band, now centered at 533 nm, and a broad band of yellow-matter fluorescence, which now peaks in the green. In addition, we now see strong fluorescence by chlorophyll *a*, centered at 685 nm. Panel (c) of the figure shows the same water excited at $\lambda' = 533$ nm. Now there is very little fluorescence by yellow matter, but the Raman band at 650 nm and the chlorophyll *a* band are quite strong. Notice that the chlorophyll *a* emission is still centered at $\lambda = 685$ nm, even though the excitation wavelength has changed.

The relative contributions of Raman scattering and fluorescence, as seen in Fig. 5.9, depend on the concentrations of yellow matter and chlorophyll *a* in the particular water sample. Because Raman emission is determined by the water itself, its characteristics are always predictable. Therefore, the Raman line can be used calibrate fluorescence measurements, or to correct remotely measured fluorescence signals for the effects of attenuation by the water; see, for example, Bristow, *et al*. (1981).

A characteristic of fluorescence by pure substances is that the emission wavelengths are independent of the excitation wavelengths. Thus chlorophyll-*a* always fluoresces in the band centered at 685 nm, regardless of whether it is excited by light at near ultraviolet, blue, green, or even red wavelengths. However, the strength of the fluorescence signal does depend on the excitation wavelength. This is because the exciting light must be absorbed by the fluorescing material before it can be re-emitted, and absorption is wavelength dependent. Therefore, for the situation seen in Figs. 5.9(b) and 5.9(c), light at $\lambda' = 450$ nm will produce stronger chlorophyll-*a* fluorescence than light at $\lambda' = 533$ nm, because absorption by chlorophyll-*a* is greater near 450 nm than near 533 nm (recall Fig. 3.7).   Fluorescence by yellow matter is more complicated, because CDOM consists of many different compounds and can vary considerably in chemical composition. In particular, the emission wavelengths for yellow matter do depend on the excitation wavelength. The substantial decrease in yellow-matter fluorescence with increasing excitation wavelength, as seen in Fig. 5.9, is attributable in large part to the exponential decrease in absorption by yellow matter with increasing λ'; recall Eq. (3.25).

If an experimenter holds the excitation wavelength λ' constant and measures the strength of the fluorescence as a function of λ, an *emission spectrum* is generated. If fluorescence is measured at a constant λ while the excitation wavelength λ' is varied, an *excitation spectrum* is generated.

The excitation spectrum is similar (but not identical) in shape to the absorption spectrum of the fluorescing substances. Because the excitation and emission spectra depend on the fluorescing substance, measurement of these two spectra has proved to be a powerful tool for the identification of fluorescing substances in natural waters. Figure 5.10 shows the general differences in excitation and emission spectra for various classes of marine algae. The additional absorption by diatoms and dinoflagellates seen in the excitation spectra (curve 1) is due to the presence of accessory pigments not found in green algae (curve 1a); note that both excitation spectra 1 and 1a
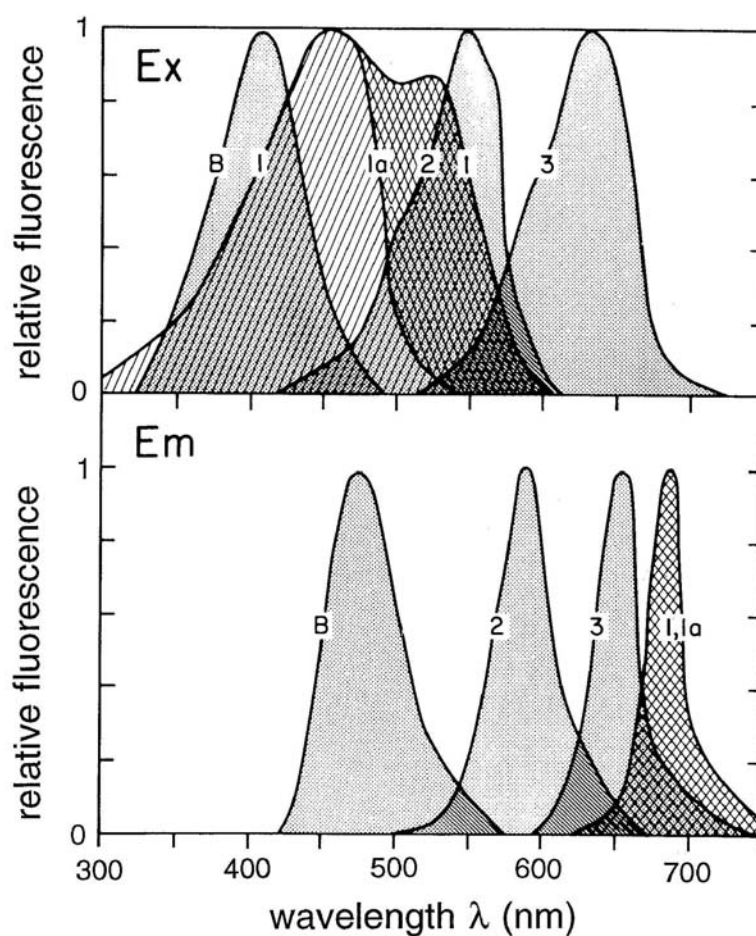
Fig. 5.10. Fluorescence excitation (top panel) and emission (bottom panel) spectra for phytoplankton. Curve 1a is for green algae; curve 1 is for diatoms and dinoflagellates; curves 2 and 3 are for cyanobacteria, cryptomonads and red algaes; and curve B is for a protein causing bioluminescence. [redrawn from Yentsch and Phinney (1981), by permission]

have the same chlorophyll emission spectra. Note also that the use of excitation and emission spectra for taxonomic classification is based on relative fluorescence signals, so that absolute radiometric calibration is not necessary. A pioneering paper on the use of fluorescence excitation and emission spectra to characterize phytoplankton populations is that of Yentsch and Yentsch (1979). A recent application of the technique to the analysis of dissolved organic matter is seen in Coble, *et al.* (1990).

Relative measurements of fluorescence as seen in Fig. 5.10 are inadequate for the quantitative needs of radiative transfer theory. In order to incorporate fluorescence into the RTE, we must construct an appropriate volume inelastic scattering function β^F, just as we did for Raman scattering. Here the superscript "F" stands for fluorescence. Towards this end, we write

$$\beta^F(z;\hat{\xi}'\rightarrow\hat{\xi};\lambda'\rightarrow\lambda) \equiv a^F(z;\lambda')f^F(\lambda'\rightarrow\lambda)\,\tilde{\beta}^F(\hat{\xi}'\rightarrow\hat{\xi}) \qquad (5.96)$$

$$(\mathrm{m}^{-1}\ \mathrm{sr}^{-1}\ \mathrm{nm}^{-1})\,.$$

Note that β^F depends on depth, because the concentration of fluorescing substances generally varies with depth. We now consider, in turn, each of the factors forming β^F.

We have *a priori* forced the depth dependence into the fluorescence absorption coefficient a^F; this is a reasonable simplification. The quantity $a^F(z;\lambda)$, with units of m^{-1}, specifies the absorption of light *by the fluorescing substance* as a function of depth and excitation wavelength. This term is usually written as the product of a concentration $C^F(z)$ and a specific absorption coefficient $a^{*F}(\lambda')$:

$$a^F(z;\lambda') = C^F(z)\,a^{*F}(\lambda') \qquad (\mathrm{m}^{-1})\,. \qquad (5.97)$$

For example, for chlorophyll fluorescence, C^F would be the chlorophyll concentration (in $\mathrm{mg\ m}^{-3}$), and $a^{*F}(\lambda')$ would be a function (with units of m^2 mg^{-1}) like those seen in Fig. 3.7.

Because photosynthesis is a quantum process, researchers using chlorophyll fluorescence as a tool for studying photosynthesis often think in terms of photons rather than energy. Accordingly, they define the *spectral fluorescence quantum efficiency function* as

$$\eta^F(\lambda'\rightarrow\lambda)\equiv$$

$$\frac{\text{the number of photons emitted at }\lambda,\text{ per unit wavelength interval}}{\text{the number of photons absorbed at }\lambda'}$$

$$(\mathrm{nm}^{-1}).\ (5.98)$$

The wavelength redistribution function $f^F(\lambda' \to \lambda)$ needed for the RTE, which is formulated in terms of energy rather than numbers of photons, is easily obtained from η^F. We need only multiply the numerator of Eq. (5.98) by hc/λ, and the denominator by hc/λ', in order to convert photon counts to energy [recall Eqs. (1.1) and (1.34)]. The result is

$$f^F(\lambda' \to \lambda) = \eta^F(\lambda' \to \lambda)\frac{\lambda'}{\lambda} \qquad (\text{nm}^{-1}). \qquad (5.99)$$

Another quantity often seen in the literature is the *quantum efficiency* (or *quantum yield*) *of fluorescence,* Φ^F, which is defined by

$$\Phi^F(\lambda') \equiv \frac{\text{the number of photons emitted at all wavelengths } \lambda}{\text{the number of photons absorbed at } \lambda'}.$$

The nondimensional $\Phi^F(\lambda')$ is related to $\eta^F(\lambda',\lambda)$ by

$$\Phi^F(\lambda') = \int_0^\infty \eta^F(\lambda' \to \lambda)\, d\lambda. \qquad (5.100)$$

The quantities η^F, f^F, and Φ^F have different forms for different substances. Figure 5.11(a) shows an example of $\eta^Y(\lambda' \to \lambda)$ for yellow matter extracted from a water sample taken in the Gulf of Mexico; the superscript "Y" reminds us that this figure is for yellow matter. Hawes (1992) made such measurements of η^Y for a variety of waters and found that the measurements were well described by a function of the form

$$\eta^Y(\lambda' \to \lambda) = A_o(\lambda')\exp\left\{-\left[\frac{\dfrac{1}{\lambda} - \dfrac{A_1}{\lambda'} - B_1}{0.6\left(\dfrac{A_2}{\lambda'} + B_2\right)}\right]^2\right\}. \qquad (5.101)$$

Here A_o (in nm^{-1}), A_1 and A_2 (dimensionless), and B_1 and B_2 (in nm^{-1}) are parameters that depend on the particular composition of the yellow matter; tabulated values are given in Hawes (1992). Figure 5.11(b) shows the fit of Eq. (5.101) to the measurements of Fig. 5.11(a).

In his studies of fluorescence by yellow matter, Hawes found $\Phi^Y(\lambda')$ to be roughly independent of λ' over the range of excitation wavelengths investigated, which was $310 \le \lambda' \le 490$ nm. Values of Φ^Y generally fell
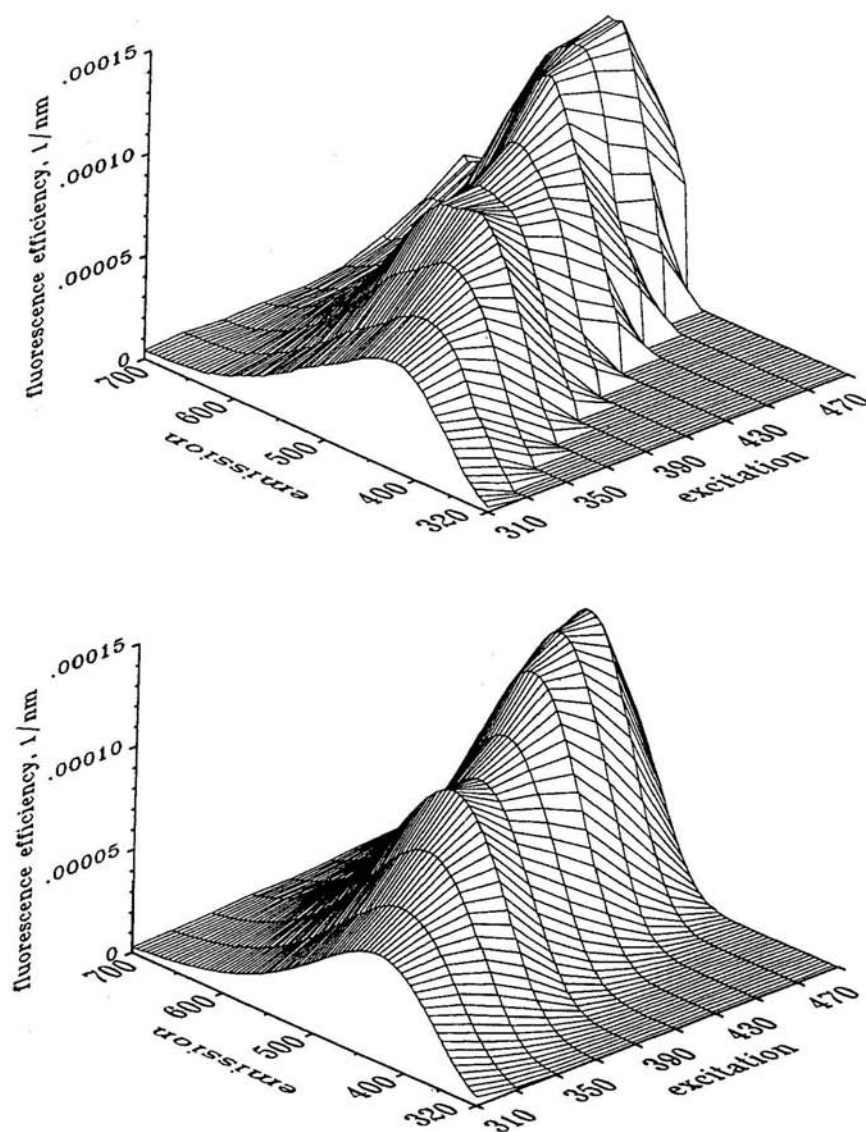
Fig. 5.11. Example of the spectral fluorescence quantum efficiency function for yellow matter, $\eta^Y(\lambda' \to \lambda)$. The excitation axis is λ', and the emission axis is λ. The top panel shows measured values for a water sample taken from the Gulf of Mexico. The bottom panel shows the fit to the measurements, as given by Eq. (5.101). [reproduced from Hawes (1992), by permission]

between 0.005 and 0.015 for the various water samples. For chlorophyll-*a* fluorescence in oceanic phytoplankton, $\Phi^C(\lambda')$ also is independent of wavelength, to a good approximation. Φ^C ranges from less than 0.01 to 0.10, with 0.01 to 0.05 being typical. Thus for every 100 photons absorbed by chlorophyll, only a few are emitted as fluorescence. Most of the others are converted to heat, although some supply the energy needed for photosynthesis. Φ^C depends in complicated ways on phytoplankton species and physiological state, as is influenced by the ambient irradiance, availability of nutrients, or the presence of toxic pollutants. Most studies of Φ^C have been made under controlled laboratory conditions, and there is much uncertainty about the behavior of Φ^C under natural conditions. The current research literature on Φ^C can be accessed via Kiefer and Reynolds (1992) and Kiefer, *et al.* (1989), and references therein.

Equation (5.99) combined with (5.101) gives us a model of the wavelength redistribution function for yellow-matter fluorescence, $f^Y(\lambda' \to \lambda)$. The corresponding quantity for chlorophyll fluorescence, $f^C(\lambda' \to \lambda)$, is usually modelled as

$$f^C(\lambda' \to \lambda) = \eta^C(\lambda' \to \lambda) \frac{\lambda'}{\lambda} \equiv \Phi^C(\lambda) \frac{\lambda'}{\lambda} g^C(\lambda') h^C \quad (\text{nm}^{-1}). \quad (5.102)$$

The λ'/λ factor converts the photon efficiency Φ^C to energy efficiency. The g^C and h^C factors seen in this equation are defined as follows:

$g^C(\lambda') =$ a nondimensional function that specifies the interval over which light is able to excite chlorophyll fluorescence,

$h^C(\lambda) =$ the chlorophyll fluorescence wavelength emission function, with units of nm^{-1},

For chlorophyll, only wavelengths in the region ~370 nm to ~690 nm can excite fluorescence. We therefore define

$$g^C(\lambda') \equiv \begin{cases} 1 & \text{if } 370 \le \lambda' \le 690 \text{ nm}, \\ 0 & \text{otherwise.} \end{cases} \quad (5.103)$$

The emission function $h^C(\lambda)$ is reasonably well approximated by a Gaussian:

$$h^C(\lambda) = \frac{1}{\sqrt{2\pi}\, \sigma^C} \exp\left[-\frac{(\lambda - \lambda_o^C)^2}{2(\sigma^C)^2} \right] \quad (\text{nm}^{-1}), \quad (5.104)$$

where

$\lambda_o^C =$ 685 nm is the wavelength of maximum emission,

$\sigma^C =$ 10.6 nm is the standard deviation of the Gaussian; 10.6 nm corresponds to a value of 25 nm for the full width at half maximum of the emission band.

Finally, for both yellow-matter and chlorophyll fluorescence, the phase function for the emitted radiance is commonly taken to be isotropic:

$$\widetilde{\beta}^F(\hat{\xi}' \to \hat{\xi}) = \widetilde{\beta}^F(\psi) = \frac{1}{4\pi} \quad sr^{-1}. \tag{5.105}$$

Strictly speaking, the use of an isotropic phase function is incorrect. It is known both from theoretical considerations (e.g. Kerker, 1977) and from measurements of fluorescence from dyes contained within small latex spheres (e.g. Kratohvil, *et al.,* 1978 and Lee, *et al*., 1978) that the phase function for fluorescent *particles* is *not isotropic.* Measurements on monodisperse latex spheres (Lee, *et al*., 1978) showed the phase function of the fluoresced light to be symmetric about $\psi = 90°$, and an order of magnitude greater near $\psi = 0°$ and $\psi = 180°$ than at $\psi = 90°$. However, the excitation-to-emission time involved in chlorophyll fluorescence is long compared to the rotational diffusion time of the fluorescing molecules, and the internal redistribution of energy within an excited chlorophyll molecule is so complex, that the fluoresced photon, once emitted, is often nearly uncorrelated with the absorbed photon. Laboratory measurements of chlorophyll fluorescence by Gordon (1993) support the use of Eq. (5.105). (The time lags associated with the fluorescent dyes mentioned above are not known but are presumed to be much shorter.)

We now have at hand all of the pieces required to assemble β^F in Eq. (5.96), for either yellow matter or for chlorophyll. It should be clear that the above analyses can be repeated for any other fluorescing substance, such as a pollutant. It is necessary only to conjure up specific absorption coefficients, wavelength redistribution functions, etc., as are appropriate for the substance under consideration.

As an internal consistency check on the model just developed for chlorophyll fluorescence, let us rewrite Eq. (5.96) as

$$\beta^C(z;\hat{\xi}' \to \hat{\xi}';\lambda' \to \lambda) \equiv b^C(z;\lambda' \to \lambda) \, \widetilde{\beta}^C(\hat{\xi}' \to \hat{\xi}) ,$$

[recall Eqs. (5.12) and (5.86)]. In the terminology of Section 5.3, $b^C(z;\lambda' \to \lambda)$ is the *volume chlorophyll-fluorescence scattering coefficient*, with units of m^{-1} nm^{-1}. Then the *chlorophyll-fluorescence absorption*

coefficient $a^C(z;\lambda')$, which measures how much of the radiance (at depth z) at λ' is lost to all other wavelengths λ, is given by [recall Eqs. (5.13) and (5.88)]

$$a^C(z;\lambda') \equiv \int_\Lambda b^C(z;\lambda' \to \lambda)\, d\lambda$$

$$= \int_\Lambda C(z)\, a^{*C}(\lambda')\, \Phi^C g^C(\lambda')\, h^C(\lambda)\, d\lambda \qquad (5.106)$$

$$= a_C(z;\lambda')\, \Phi^C g^C(\lambda') \qquad (\mathrm{m}^{-1}).$$

The quantity $a_C(z;\lambda') = C(z)a^{*C}(\lambda')$ is the absorption by chlorophyll at depth z and wavelength λ'. The last equation in (5.106) shows that the energy lost in the inelastic process is just the energy absorbed times the fraction converted to longer wavelengths. The quantity $a^C(z;\lambda')$ is often called the "fluorescence coefficient." Note that a measured value of the beam attenuation $c(z;\lambda')$, which includes the contribution by chlorophyll absorption, $a_C(z;\lambda')$, fully accounts for the effects of fluorescence. A fraction $a_C\Phi^C g^C$ is converted to other wavelengths and the remaining fraction, $a_C(1 - \Phi^C g^C)$, is converted to heat or chemical energy.

Use of the above formalism in numerical simulations of chlorophyll fluorescence can be traced back at least as far as Gordon (1979). Recent work by Haltrin and Kattawar (1993) used the same functional form for η^Y as that seen above for η^C. Detailed, quantitative information like that seen in Fig. 5.11 is just now becoming available for substances other than chlorophyll, and much work remains to be done in learning about the variability of η^F in natural waters.

5.16 Bioluminescence

Only one term in the radiance transfer equation (5.20) has not yet been discussed in detail, and that is the true emission, or true internal source, term L_*^S.

Light-emitting marine organisms are ubiquitous in the world's oceans. They range in size from bacteria to fish, and they are found from the sea surface to its bottom and from the arctic to the equator. The very presence of sensitive eyes in fish living near the sea floor, where sunlight never reaches, hints at the existence and importance of light at even the greatest depths. Possible ecological roles for self-emitted light include communication for courtship or schooling, attraction of prey, and escape from predators. For example, Widder (1992) shows a remarkable sequence

of photographs in which a disturbed copepod *Euaugaptilus magnus* emits a luminous blob of material that remains behind as the dark copepod flees. Clark, *et al.* (1962) measured the light emitted by *E. magnus* as having an irradiance of 1.5×10^{-9} W m^{-2} at a distance of 1 m. This irradiance is well above 10^{-12} W m^{-2}, which is the estimated threshold of sensitivity of the eyes of some fish (Denton and Warren, 1957).

We already have commented in Section 5.5 that a bioluminescent light source isotropically emitting spectral radiant power of $S_o(\lambda)$ W m^{-3} nm^{-1} into 4π sr can be included in the radiance transfer equation as a source term of the form

$$L_*^S(z;\hat{\xi};\lambda) = S_o(z;\lambda)\,\tilde{\beta}^S(\hat{\xi}) = \frac{S_o(z;\lambda)}{4\pi} \qquad (\text{W m}^{-3}\ \text{sr}^{-1}\ \text{nm}^{-1}).(5.107)$$

Quantitative studies of bioluminescence, as are relevant to the needs of hydrologic optics, are just beginning. Nevertheless, some quantitative information about the nature of the power emission function $S_o(\lambda)$ is available. Widder, *et al.* (1983) examined the shape of $S_o(\lambda)$ for 70 marine species ranging from bacteria to fish. Figure 5.12 illustrates the range of shapes of $S_o(\lambda)$ encountered in her study. The wavelengths of maximum emission, λ_{max}, and the full-width at half-maximum of the emission band $\Delta\lambda_{FWHM}$, are indicated in the figure caption. The range of λ_{max} was 439 nm to 574 nm, with an average over all species of $\lambda_{max} = 483$ nm. The bandwidths $\Delta\lambda_{FWHM}$ ranged from 26 nm to 100 nm, with an average of about 75 nm. Not surprisingly, these wavelength bands coincide with the wavelengths where sea water is most transparent.

The magnitude of $S_o(\lambda)$ shows more variability than its shape. We first note that most bioluminescent organisms emit light only when they are disturbed. The most common light-inducing disturbance is mechanical stimulation, as when an organism is entrained into a ship's turbulent wake or feels a pressure wave caused, perhaps, by an approaching fish. Flashing lights, electrical fields, and chemical irritants are also known to induce bioluminescence. [Lapota, *et al.* (1986) give an interesting description of bioluminescence induced by an ordinary flashlight.] When disturbed, organisms emit a flash of light that may last from tens of milliseconds to several seconds. The exception to this statement is certain bacteria, which are able to emit light continuously.

A common measure of $S_o \equiv \int_\Lambda S_o(\lambda)d\lambda$ is the number of photons emitted per second by a disturbed organism. Typical values are $S_o = 10^4$ photons s^{-1} cell^{-1} for bacteria, and 10^9 to 10^{11} photons s^{-1} cell^{-1} for dinoflagellates; see Lynch (1978) for tabulations of S_o for 58 marine species. A quick calculation will give us a feeling for the light levels that are
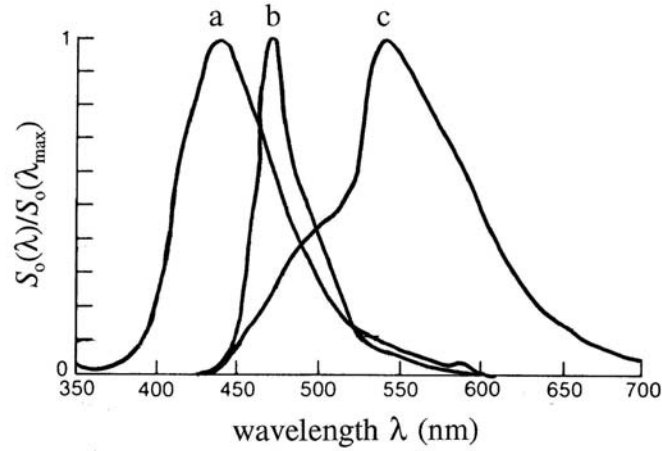
Fig. 5.12. Spectral shapes $S_o(\lambda)$ of bioluminsecence for three particular organisms: curve a, the arthropod *Scine cf. rattrayi*, λ_{max} = 439 nm, $\Delta\lambda_{FWHM}$ = 70 nm; curve b, the dinoflagellate *Pyrocystis noctiluca*, λ_{max} = 472 nm, $\Delta\lambda_{FWHM}$ = 35 nm; curve c, the bacterium *Vibrio fischeri* Y-1 strain, λ_{max} = 540 nm, $\Delta\lambda_{FWHM}$ = 81 nm. [redrawn from Widder, *et al.*, (1983), by permission]

possible. Assuming a typical concentration of 2000 cells m^{-3} of a bioluminescent dinoflagellate, with each cell emitting 5×10^{10} photons s^{-1} with an average wavelength of λ = 480 nm, and converting the photon count to energy units via Eq. (1.1), gives

$$S_o = (2 \times 10^3 \text{ m}^{-3})(5 \times 10^{10} \text{ s}^{-1}) \frac{(6.63 \times 10^{-34} \text{ J s})(3 \times 10^8 \text{ m s}^{-1})}{480 \times 10^{-9} \text{ m}}$$

$$\approx 4 \times 10^{-5} \text{ W m}^{-3}.$$

If this power is generated in a single sphere of volume 1 m^3 (for example, in a turbulent eddy), then the surface of the sphere receives an irradiance of order 10^{-5} W m^{-2}. Reference to Table 1.4 shows this irradiance to be greater than that of a clear, starry night, but much less than that of a bright, moonlit night. The 10^{14} photons s^{-1} m^{-3} used in this estimate is in line with observations. For example, Lapota, *et al.* (1988) measured values of $1-5 \times 10^{14}$ photons s^{-1} m^{-3} during periods of high bioluminescence in the Arabian Sea.

Although disturbed organisms can provide enchanting light shows, some of the most spectacular displays are caused by bacteria near the sea

surface. The large numbers of bacteria and their ability to emit light continuously more than make up for their low photon emittance per cell. The Indian Ocean and Arabian Sea are known for their horizon-to-horizon displays of luminous "milky seas," which can generate enough light for reading on the deck of an otherwise dark ship. Mariners' logs contain many such reports; see Kelly and Tett (1978) for examples. Lapota, *et al.* (1988) give quantitative observations of a "milky sea" event.

Bioluminescence also occurs in terrestrial organisms from fungi to fireflies but, curiously, is known to occur in only one freshwater species (a New Zealand mollusk). A useful collection of papers on bioluminescence is found in Nealson (1981).

Bradner, *et al.* (1987) examined physical sources of light in the ocean. They estimate that near the sea surface, Cherenkov radiation from cosmic rays generates a photon irradiance of order 10^7 photons $m^{-2} s^{-1}$; this value decreases exponentially with depth. They also estimate that Cherenkov radiation from relativistic electrons emitted in the decay of naturally occurring ^{40}K generates about 1.2×10^6 visible photons $m^{-2} s^{-1}$ at all depths in very clear waters. Their nighttime measurements to depths of 4300 m in clear waters near Hawaii showed a typical background "glow" of order 10^7 photons $m^{-2} s^{-1}$, which includes bioluminescence as well as sources such as ^{40}K decay. Thus it is never completely dark at even the greatest depths, even though no solar photons are present. If we assume photons of wavelength 450 nm, then 10^7 photons $m^{-2} s^{-1}$ corresponds to 4×10^{-12} W m^{-2} which, interestingly, is just above the estimated threshold for detectability by some deep-sea fish.

5.17 Historical Notes

Lommel (1889) appears to be the first to derive a form of the RTE. He clearly described how light is both absorbed and scattered *from* a volume element within a translucent medium, and how all of the other volume elements within the medium scatter light *into* the element under consideration. He defined quantities corresponding to *a, b* and *c*, assumed an isotropic phase function (in modern terminology), and developed an integral equation to account for the gains to and losses from the light field at a given point owing to absorption and scattering throughout the medium. Lommel's equation corresponds closely to our integral form (5.30) for the case of homogenous, source-free media.

Lommel went on to obtain approximate solutions to his equation (using a successive-order-of-scattering approach, through first order) for

plane-parallel media. He then used these approximate solutions to study how light diffusely reflected by translucent bodies depends on the angles of incidence and reflection, on ω_o, on the thickness of the medium, and on the nature of the incident lighting (collimated or diffuse). He even showed that the diffuse light field can achieve a maximum at some finite distance beneath the surface; such behavior was seen in Fig. 5.3. His paper finishes with a favorable comparison of predicted and measured reflectances for marble, paper, and porcelain. Lommel's pioneering and highly competent work, published in a major journal, was either unappreciated or simply forgotten. Consequently, the astrophysicists Schuster and Schwarzschild are commonly recognized as being the founding fathers of radiative transfer theory.

A special case of the two-flow equations was first derived by Schuster (1905) in a study of stellar spectra. These equations have been rediscovered and reformulated many times since in studies ranging from astrophysics to oceanography to paint technology. Particular studies almost always begin with assumptions about the phase function or about the radiance distribution, in which case the derived forms of the two-flow equations are special cases of the general equations obtained in Section 5.10. For example, Schuster assumed that the phase function was symmetric about $\psi = 90°$ (as is the Rayleigh phase function, for example) and that the radiance was isotropic within each hemisphere, although the upward and downward hemispheres could have different radiance values. For his application to stellar atmospheres, these were reasonable assumptions. Even so, he explicitly stated that "This supposition [about the radiance distribution] is obviously incorrect,...." He also included internal source terms to account for the blackbody radiation of the luminous gas. Schuster's two-flow equations correspond to Eqs. (5.54) and (5.55) with $a_u = a_d = 2a$ and $b_{du} = b_{ud} = 2b_b$. Schuster recognized that the correct form of the two-flow equations was more complicated. Indeed, he wrote that [Schuster (1905), quoted by permission] "The complete investigation leads to equations of such complexity that a discussion becomes impossible, and I shall only use the solution obtained under the simplified conditions to deduce certain consequences which cannot be affected by the assumption made." He then went on to show how the presence of the scattering terms in the two-flow equations can account for both dark and bright lines in stellar spectra, whereas the spectrum would be that of a blackbody if scattering is ignored. His work well illustrates how much information can be squeezed from the two-flow equations, even though in general they cannot be solved for the irradiances. This classic paper is recommended reading even after almost a century.

Schwartzschild (1906) used both Schuster's two-flow irradiance equations and a differential-equation form of the RTE in a landmark study of the sun's atmosphere. However, he considered only the processes of absorption and blackbody emission. His form of the RTE is equivalent to Eq. (5.22) with $L_*^{E} = 0$ – quite a simplification! Schwartzschild's real contribution was his introduction of the concept of radiative equilibrium, in which energy transport by electromagnetic radiation dominates transport by convection or conduction. By combining his simple forms of the radiative transfer equations with the hydrostatic equation for fluids, he was able to deduce the basic thermodynamic structure of the sun's atmosphere and, in particular, to explain its stability.

Not until King (1913) published a lengthy and rather mathematical paper on atmospheric scattering and absorption did anyone treat radiative transfer with the physical and mathematical sophistication seen in Lommel's 1889 paper. King developed an integral form of the RTE that is equivalent to our Eq. (5.28). He went on to solve his equation under various assumptions, such as that of isotropic scattering, and in so doing he reproduced some of Lommel's results from 24 years earlier.

King's rigorous treatment of radiative transfer in scattering and absorbing media caught the attention of Duntley, who did pioneering work in atmospheric and underwater optics during and after the second world war. His review paper on the mathematics of turbid media (Duntley, 1943) discusses both Schuster's and King's work.

During the summers of 1950 and 1951 a young undergraduate student named Preisendorfer worked with Duntley on atmospheric and underwater visibility problems at Lake Winnepesaukee, New Hampshire, USA. Thus was planted the seed that eventually grew into Preisendorfer's monumental works of 1965 and 1976. His goal in these books was to place hydrologic optics on a firm mathematical foundation, and he succeeded. Moreover, Preisendorfer, a mathematician, recognized the power of invariant imbedding theory and of other analytical methods both as tools for solving the RTE and as a framework for developing deep insights into the internal structure of radiative transfer theory. These matters will be discussed in Chapters 7-9.

In 1979, a postdoctoral student doing numerical modeling of water waves struck up a conversation with the occupant of the office next door. And so began the collaboration of computer modeler and pencil-and-paper theoretician that led eventually to the present book.

5.18 Problems

5.1. Show that Gershun's law can be obtained by adding together the two-flow irradiance equations.

5.2. Solving Eq. (5.35) for a gives

$$a = -\frac{1}{E_o} \frac{d(E_d - E_u)}{dz} + \frac{E_o^S}{E_o}.$$

This equation seems to imply that the presence of an internal source ($E_o^S > 0$) at the wavelength of interest would give an absorption value *greater* than would be obtained if there were no source present ($E_o^S = 0$). This is contrary to the arguments presented in Section 5.14. Resolve this paradox in 25 words or less.

5.3. Assume that the upper three meters of the ocean contain a uniform distribution of continuously bioluminescing bacteria, with no bacteria below $z = 3$ m. There are 10^{11} cells m^{-3}, each emitting 10^4 photons s^{-1} cell^{-1}. The water is Jerlov type IB, and the wind speed is 5 m s^{-1}. Compute the irradiance E_u that leaves the water surface, assuming that all photons have $\lambda = 550$ nm and that the underwater radiance distribution is described by a cardioidal distribution with parameter $C = -0.7$. How does this irradiance compare to that of the full moon on a clear night?

5.4. Derive Eq. (5.68) from Gershun's law.

5.5. Consider an infinite (in all directions), homogeneous medium with a single isotropically emitting point source of light located at the origin of a spherical (r, θ, ϕ) coordinate system. We can think of the source as being a sphere of some small radius r_o, which has a spectral surface radiance of magnitude (constant in time) $L(r_o, \theta, \phi) \equiv L_o$, with all of the photons heading in the $\hat{\xi}$ (radially outward) direction. Furthermore, assume that the medium scatters isotropically: $\tilde{\beta} = 1/4\pi$.
(a) Using symmetry arguments, show that the general RTE (5.19) reduces to

$$\cos\gamma \frac{\partial L(r;\gamma)}{\partial r} + \frac{\sin\gamma}{r} \frac{\partial L(r;\gamma)}{\partial \gamma} = -cL(r;\gamma) + \frac{\omega_o}{2} \int_0^\pi L(r;\gamma') \sin\gamma' d\gamma' \qquad (5.108)$$

for this problem. Here γ is the angle between $\hat{i}_1$ and $\hat{\xi}$ at location $\vec{x} =$

(r,θ,ϕ). The reduction of $\hat{\xi}$ and the change of variables is not trivial, so be careful.

(b) Consider the case of absorption only: $c = a$ and $\omega_o = 0$. The integral form of the RTE, Eq. (5.30), suggests that we seek a solution of the form

$$L(r;\gamma) = L_o \exp\left[-\frac{a(r - r_o)}{\cos\gamma}\right]$$

for Eq. (5.108). Show that this $L(r;\gamma)$ satisfies Eq. (5.108) only if $\gamma = 0$, i.e. only if the photons continue to travel in the radial direction. Note that this solution satisfies the boundary conditions $L(r_o,\theta,\phi) = L_o$ and $L \to 0$ as $r \to \infty$.
(c) Now try to find a function $L(r;\gamma)$ that satisfies Eq. (5.108) and the boundary conditions when $\omega_o \neq 0$. If you find this difficult, keep in mind that this is one of the geometrically simplest problems in radiative transfer theory.

5.6. If finding the radiance in problem 5.5(c) was too hard for you, try finding the *irradiance* due to a point source. Once again, consider an infinite, homogeneous water body with an isotropic point source at the origin, but let the phase function remain arbitrary. As in problem 5.5, we can regard the source as a small sphere of radius r_o. Now the spectral radiant emittance of the sphere is taken to be

$$M(r_o) = \frac{\Phi_o}{4\pi r_o^2} \quad \left(\frac{W}{m^2\,nm}\right),$$

where Φ_o is the spectral power emitted by the source at some wavelength λ.
(a) Define the *radial component of the vector irradiance* as

$$E_r(r) \equiv \left(\vec{E}(r)\right)_r \equiv 2\pi \int_0^\pi L(r,\gamma)\cos\gamma\,\sin\gamma\,d\gamma$$

$$= E_{+r} - E_{-r}.$$

Here γ is defined relative to the radial direction $\hat{r}$ as in problem 5.5, and not relative to $\hat{i}_3$, which defines θ. E_r is like the vertical component of the vector irradiance defined in Eq. (1.28), except that now it is the radial direction, rather than the vertical direction, that is involved. E_r is thus the difference in the plane irradiances measured by instruments pointed toward and away from the origin. Use symmetry arguments to show that the

divergence law for irradiance, Eq. (5.36), now can be written as

$$\frac{dE_r(r)}{dr} + \frac{2\,E_r(r)}{r} = -a\,E_o(r).$$ (5.109)

(b) Show that Eq. (5.109) is also obtained by integrating Eq. (5.108) over all directions.

(c) Now define the *radial mean cosine* $\bar{\mu}_d$ as

$$\bar{\mu}_r(r) \equiv \frac{E_r(r)}{E_o(r)}.$$

Note that $\bar{\mu}_d$ is just like $\bar{\mu}_d$, except that it measures the mean cosine of photon directions relative to the radial direction, rather than relative to the nadir direction. Show that Eq. (5.109) has the solution

$$E_r(r) = \frac{\Phi_o}{4\pi r^2}\,e^{-a\bar{r}},$$ (5.110)

where

$$\bar{r} \equiv \int_{r_o}^{r} \frac{dr'}{\bar{\mu}_r(r')}$$

is the *mean light path*. Note that if there is no scattering, all unabsorbed photons continue to travel radially outward from the source, in which case γ = 0 and $\bar{\mu}_d$ = 1. Note that the *form* of Eq. (5.110) is the same for any phase function. The effects of the phase function are parameterized in terms of $\bar{\mu}_r$. Just as with $\bar{\mu}_d$, the determination of $\bar{\mu}_r$ requires the measurement of both plane and scalar irradiances and is therefore difficult. Maffione, *et al.* (1993) have extended this solution to horizontally stratified water and shown how to recover *a* from plane irradiance measurements made *in situ* using an isotropic light source.

5.7 Parallel the analysis of problem 5.6 to find the irradiance generated by an infinitely long *line* source in an infinite, homogeneous medium with an arbitrary phase function. You can envision the line source as being an infinitely long fluorescent light of radius r_o that emits a spectral power Φ_o per unit length.

5.8 Consider the case of isotropic scattering, $\beta = b/4\pi$. Evaluate the corresponding forward and backward scattering functions f_{uu}, b_{du}, etc.,

expressing your answers in terms of $\bar{\mu}_d$ and $\bar{\mu}_u$. Write the two-flow equations in terms of a and b for the case of isotropic scattering. What additional simplifications result if the radiance is also isotropic, $L(\theta,\phi) = L_o$?

5.9. What wavelength λ' contributes most strongly to the Raman-scattered light at $\lambda = 589$ nm, as discussed in Fig. 5.8?

5.10   How does the number of visible photons generated by blackbody radiation from deep ocean water at a temperature of 2°C compare with the number generated by the decay of ^{40}K?